Delft University of Technology

Design and evaluation of a constraint-based head-up display for helicopter obstacle avoidance

Friesen, Daniel; Borst, Clark; Pavel, Marilena D.; Stroosma, Olaf; Masarati, Pierangelo; Mulder, Max

Important note
To cite this publication, please use the final published version (if applicable).
Please check the document version above.

Design and Evaluation of a Constraint-Based Head-Up Display for Helicopter Obstacle Avoidance

Daniel Friesen,[*] Clark Borst,[†] Marilena D. Pavel,[‡] and Olaf Stroosma[§]
Delft University of Technology, 2629 HS Delft, The Netherlands
Pierangelo Masarati[¶]
Polytechnic University of Milan, 20156 Milan, Italy
and
Max Mulder[**]
Delft University of Technology, 2629 HS Delft, The Netherlands

This paper investigates the effect of employing different display design principles for human–machine interaction in helicopters. Two obstacle avoidance support displays are evaluated during low-altitude forward flight. A baseline head-up display is complemented either by a conventional advisory display or a constraint-based display inspired by ecological interface design. The latter design philosophy has only been sparsely applied in the helicopter domain. Twelve helicopter pilots participated in an experiment in a research flight simulator. We found no significant effects of the displays on objective performance measures. However, there was a trend of decreasing pilot workload and increasing situation awareness when employing the support displays, as compared to the baseline display. The constraint-based display had the largest positive effect and increased the resilience of the pilot–vehicle system toward unexpected events when considering the safety of the flown trajectories. Pilots preferred the advisory display in nominal situations and the constraint-based display in off-nominal situations, reproducing similar findings from research in the fixed-wing domain. This experiment showed the potential of the developed constraint-based display to improve subjective pilot ratings, pilot preference, and safety during unexpected events. Future research will investigate more complex scenarios with longer time frames, possibly eliciting more divergent effects of different display design principles.

Nomenclature

d_0	=	display design variable; minimum distance for which the maneuver constraints are valid, m
F	=	F distribution, used in analysis of variance test statistics
g	=	gravitational constant, m/s^2
h_{limit}	=	maximum altitude difference achievable within d_0 at the given forward speed V, m
k	=	τ-maneuver coupling constant
m	=	mass of the helicopter, kg
$P_{\text{available}}$	=	available maneuvering power available at the given forward speed V, W
P_{max}	=	maximum engine power, W
P_{req}	=	steady-state power required at the given forward speed V, W
p	=	probability value of employed statistical tests
p_{reserve}	=	power reserve ratio for maneuvering, tail rotor power consumption, and overcoming additional maneuver-induced aerodynamic resistance
R^2	=	coefficient of determination of a prediction
T	=	τ-maneuver time, s
t	=	time, s
t_{end}	=	τ-maneuver end time, s
t_{start}	=	τ-maneuver start time, s
$\hat{t}$	=	τ-maneuver normalized time
V	=	forward speed of the helicopter, m/s
x_{maneuver}	=	distance between maneuver onset and point of origin of resulting flight path γ_{max}, m
x_τ	=	pilot reaction distance, m
α	=	significance level of statistical tests
γ	=	flight-path angle, rad
γ_{end}	=	τ-maneuver flight-path angle end value (zero, per definition), rad
γ_{gap}	=	τ-maneuver flight-path angle gap, rad
γ_{limit}	=	maximum effective climb angle, rad
γ_{max}	=	maximum climb angle, rad
γ_{maneuver}	=	τ-maneuver flight-path angle, rad
γ_{obstacle}	=	visual angle between the top of an obstacle's safety zone and the horizon, rad
γ_{start}	=	τ-maneuver flight-path angle start value (negative, per definition), rad
$\dot{\gamma}$	=	flight-path angle rate of change, rad/s
$\dot{\gamma}_{\text{max}}$	=	maximum flight-path quickness, rad/s
τ_{guide}	=	τ-maneuver intrinsic constant-acceleration guide, s
τ_{maneuver}	=	τ-maneuver momentary time to contact, s
τ_p	=	pilot reaction-onset delay, s
χ^2	=	chi-squared distribution, used in two-way Friedman test statistics
Ω	=	main rotor speed, rad/s

---

*Ph.D. Student, Section Control and Simulation; also Department of Aerospace Science and Technology, Polytechnic University of Milan, 20156 Milan, Italy; d.friesen@tudelft.nl. Student Member AIAA.
†Assistant Professor, Section Control and Simulation; c.borst@tudelft.nl. Member AIAA.
‡Associate Professor, Section Control and Simulation; m.d.pavel@tudelft.nl.
§Researcher, Section Control and Simulation; o.stroosma@tudelft.nl. Senior Member AIAA.
¶Professor, Department of Aerospace Science and Technology; pierangelo.masarati@polimi.it. Member AIAA.
**Professor, Section Control and Simulation; m.mulder@tudelft.nl. Associate Fellow AIAA.

I. Introduction

THIS paper investigates the effect of an advisory and a constraint-based obstacle avoidance display on safety, task performance, pilot workload, situation awareness, control activity, and control strategy during forward flight. It also investigates whether the switch of preference from advisory systems to constraint-based systems

during off-nominal events, which has been observed in the fixed-wing domain, can be observed in the helicopter domain as well, even though the vehicle dynamics and control strategies differ between helicopters and fixed-wing aircraft.

Helicopter operations still face a higher accident rate per flight hour when compared to fixed-wing operations. The helicopter accident rate in the United States between 2016 and 2020 is estimated to be 3.45 accidents per 100,000 flight hours [1]. The "Annual Safety Review 2019", published by the European Union Aviation Safety Agency, determines the European fixed-wing commercial air transport accident rate at 0.19 accidents per 100,000 flight hours [2]. Although these metrics are not directly comparable, given the very different mission structure and risks associated with helicopter versus commercial fixed-wing aircraft operations, these numbers nonetheless act as a motivation to aim for higher safety and lower accident rates in the helicopter domain.

According to a report of the European Helicopter Safety Team, incorrect or flawed pilot judgment and actions contribute to 68% of the 487 helicopter accidents analyzed. Loss of situation awareness (by being unaware of obstacles in the flight path; also caused by bad visibility/weather) can be an enabling factor for these judgments. In their report, loss of situation awareness is attributed to more than 30% of accidents, being the fourth-largest factor after safety management (49%) and ground duties (39%). Loss of situation awareness can be caused, for example, by flying in a degraded visual environment, which could increase the chance of incorrect or flawed pilot judgment and actions [3,4].

A contributing factor to this lower level of safety is the large variability within many helicopter missions, like helicopter emergency medical services (HEMSs) or search and rescue (SAR). Pilots are frequently required to make safety-critical decisions while facing unexpected or off-nominal situations like a change of mission requirements, adverse weather conditions, or obstacles to mission success that were unaccounted for during mission planning. In these situations, improving the resilience of the pilot–vehicle system against unsafe outcomes is crucial.

One way of increasing resilience is developing and employing novel automation systems that support the pilot in these safety-critical situations. Head-up display (HUD) technology has been applied successfully to improve the usable cue environment level by supplying the pilot with an additional perspective overlay based on data recorded by onboard sensor suites and/or offline maps [5–7]. When developing novel automation systems, there are drawbacks to consider: guidance systems (e.g., maneuver cue-following symbology) applied in addition to existing HUD symbology suffered from sensory overload because the two-dimensional cues were typically added on top of the augmented outside view [8]. In this case, the outside view was distracting the pilot from the two-dimensional cue-following task. Current concepts of obstacle avoidance systems provide maneuvering advice [9], increase the perception of obstacles by magnifying them visually [6,10], or provide combined visual/auditory cues [11]. Maneuver-following cues have been implemented recently in a HUD as a tunnel-in-the-sky or virtual leading aircraft [12].

It is a challenge, however, to develop automation systems that work well in off-nominal situations. Automation systems for nominal operations are often advisory systems, suggesting (or implementing) a specific optimal solution to the current situation. In contrast, design methodologies exist that focus on supporting human adaptive, resilient control. For example, systems based on ecological interface design (EID) aim at making the operational constraints tangible to the pilots, supporting their decision making without prescribing a specific solution [13].

Ecological interfaces aim to provide information about the controlled system and its environment such that the internal and environmental constraints on possible operator actions and system reactions become easily apparent [14,15]. Visualized constraints are physical (e.g., avoiding flight into terrain) and intentional (e.g., staying above a predetermined safe altitude) [16]. Borst et al. [17] provided an up-to-date reflection on EID, and the philosophy of applying EID principles to vehicle control has been summarized by Van Paassen et al. [13]. The crucial difference between ecological

displays and conventional advisory systems lies in the kind of information they provide to the pilot. Ecological displays provide information about possible actions and limitations, enabling the controller to choose the most appropriate action. Conventional advisory systems typically provide one specific solution or piece of advice. Flight directors, which propose a certain flight path, or helicopter hover displays with cue symbology, which provide a specific maneuver specification for the pilot to follow, are examples of conventional advisory displays.

As of now, ecological design principles have only been sparsely applied in the helicopter domain, for example, for shipboard landing [18]. Research in the domain of fixed-wing passenger aircraft by Borst et al. [19] has shown that ecological interfaces are less desired by fixed-wing pilots during obstacle avoidance tasks in nominal flight situations. Conversely, in off-nominal situations including system failures, pilots prefer ecological interfaces [19]. There are some differences between the investigated fixed-wing task and helicopter obstacle avoidance maneuvers: Borst et al. [19] did not consider nap-of-the-Earth operations (something which is much more relevant in the helicopter domain) but rather a terrain avoidance task while piloting a model of a Cessna Citation 500. While the terrain avoidance decision-making in a Cessna Citation 500 can usually take tens of seconds or even minutes, the decision process often has to be much faster in the helicopter domain, especially when low-altitude flight situations are considered. Also, the task of controlling a helicopter tends to be more focused on hands-on short-term stabilization and control, whereas the control of fixed-wing passenger aircraft is typically more stable in the short term, freeing some cognitive resources to focus on more elaborate displays. These differences in typical vehicle dynamics and short-term attention requirement can reduce the positive preference effect of employing the constraint-based display, as compared to the advisory display.

In October and November of 2019, a human-in-the-loop experiment was conducted in the simulation, motion, and navigation (SIMONA) research simulator at Delft University of Technology. During the experiment, two different HUD obstacle avoidance displays were evaluated in different visibility conditions and during unexpected off-nominal events. They were compared with a baseline HUD without any maneuver cueing. One display is a conventional "advisory display," which provides a discrete maneuver suggestion to the pilot. The other one is a "constraint-based display," which takes inspiration from ecological interface design by visualizing the flight-path constraint of a pull-up and climb-over maneuver to the pilot via a maximum effective climb angle. Employing constraint-based displays that decouple the internal constraints (e.g., performance and model dynamic restrictions) and external constraints (e.g., position and height of obstacles) of the vehicle and its environment might improve the resilience of the pilot–vehicle system to unexpected situations and subsystem faults.

The obstacle avoidance scenario is chosen for three reasons. First, external environment awareness plays a major role in historic helicopter accidents [3,4]. Displays that support pilots in avoiding approaching obstacles can reduce the danger of collision. Second, the required climb-over maneuver can be encountered in many different helicopter missions: be it in military missions (nap-of-the-Earth flying) or civil missions (approach to an unknown landing spot during HEMS operations or low-altitude flight during SAR missions). It is therefore applicable to a broad range of operational environments. Lastly, it resembles the obstacle avoidance task employed by Borst et al. [19], which will enable the comparison of the high-level results between helicopter and fixed-wing display effects.

The paper is structured as follows. Section II discusses the design of the displays. The experiment methodology is elaborated on in Sec. III. Section IV shows the results, which are discussed in Sec. V. This section also contains an outlook to possible improvements and future research activities. Section VI contains the conclusions to this work.

II. Display Design

This section elaborates on the employed displays. First, the baseline HUD and the obstacle detection and contour drawing system are
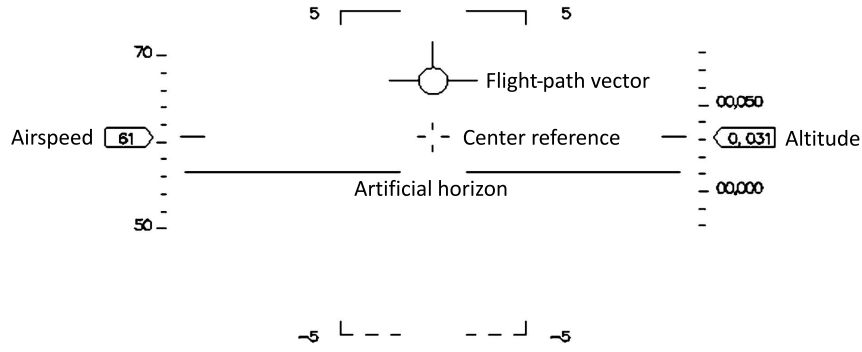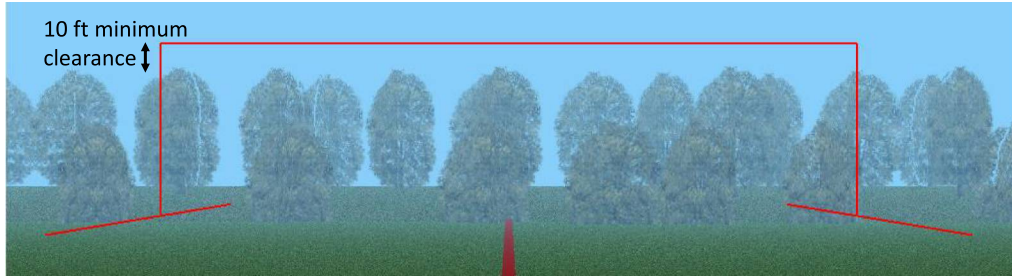
Fig. 1 Baseline HUD elements.

Fig. 2 Red box around an approaching obstacle in the HUD, drawn by the obstacle detection and contour drawing system.

explained. The following subsection details the maneuver constraint calculation on which both displays are based. Then, the two employed displays (advisory and constraint-based) are elaborated upon. The Messerschmitt–Bölkow–Blohm Bo105 Helicopter serves as a reference for power calculations [20]. In the last subsection, the employed displays are classified with respect to existing helicopter display systems.

A. Baseline Head-Up Display

The baseline HUD is a control variable, shown to the pilot in every experiment condition, depicted in Fig. 1. It is projected on top of the outside visuals, and no helmet-mounted technology is used. It consists of the following elements: 1) an artificial horizon and conformal pitch ladder, indicating every 5 deg above and below the horizon line; 2) an aircraft reference point, indicating the direction in which the helicopter's nose is pointing; 3) an altimeter in feet; 4) a speed tape in knots; 5) a flight-path vector; and 6) an obstacle detection and contour drawing system, explained in the following paragraph.

The obstacle detection and contour drawing system visualizes the minimum clearance altitude above obstacles. It superimposes a red line around the obstacle in the HUD at a distance of 10 ft, which is the minimum clearance; see Fig. 2. A clearance of 10 ft is chosen to discourage pilots to target the exact upper edge of the obstacle, which could cause dangerous "near misses" of the obstacle. Its concept is based on systems described by Münsterer et al. [6], which draw warning contours around dangerous obstacles like windmills.

B. Calculation of Internal and External Constraints

Both support displays are based on the maximum "effective" climb angle γ_{limit} within a certain longitudinal distance d_0. Its calculation takes into account the maximum steady-state climb angle γ_{max} based on available power, an assumed pilot reaction-onset delay τ_p, and model dynamic restrictions. Note that γ_{limit} is determined by calculating the maximum height gain h_{limit} that can be achieved within a distance of d_0. Figure 3 depicts the parameters of the climb-over maneuver constraint calculation, with an obstacle depicted at a distance of d_0. Table 1 contains constant parameter values for the following calculation.

The distance d_0 is a display design parameter. It represents the minimum distance to an obstacle at which the calculated maneuver constraint is still valid. If an obstacle is further away than d_0, γ_{limit} is a
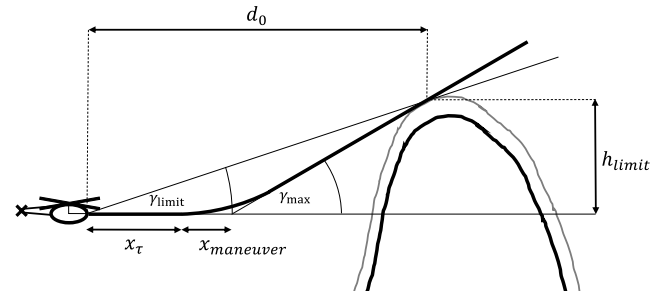

Fig. 3 Display parameters of the climb-over maneuver over an obstacle's safety zone.

conservative estimate. With an obstacle directly at d_0, it represents the exact maneuver limit, taking into consideration the pilot and model delays. At distances smaller than d_0, it overestimates the maneuver possibilities of the helicopter before reaching the obstacle.

To determine the steepest climb angle γ_{max}, the power required at the given forward speed P_{req} is subtracted from 80% of the maximum engine power P_{max}. The resulting speed-dependent power available $P_{\text{available}}$ is transformed into an increase in potential energy (climbing). The mass of the helicopter is assumed to be $m = 2500$ kg. Equation (1) details the calculation of γ_{max}:

Table 1   Constant parameter description and values for display constraint calculation

Parameter	Explanation	Value
P_{max}	Maximum engine power	588 kW
P_{reserve}	Power reserve ratio for maneuvering, tail rotor power consumption, and overcoming additional maneuver-induced aerodynamic resistance	20%
m	Mass of the helicopter	2500 kg
g	Gravitational constant	9.80665 m/s²
τ_p	Pilot reaction-onset delay	0.8 s [21]
$\dot{\gamma}_{\text{max}}$	Maximum flight-path quickness	5 deg/s
d_0	Minimum maneuver distance	120 m
Ω	Main rotor speed	44.4 rad/s ≈ 424 rpm

$$\tan(\gamma_{max}) = \frac{(P_{available}/mg)}{V} \qquad (1)$$

At a forward speed of 60 kt, the power required is approximately 202 kW, based on a main rotor torque of 4556 N/m and a main rotor speed of $\Omega = 44.4$ rad/s. The remaining available power to climb is approximately 268 kW. This results in a climb rate of 10.94 m/s or a maximum climb angle $\gamma_{max} = 19.5$ deg.

The helicopter cannot immediately attain this climb angle. The distance over which the helicopter can climb with γ_{max} is reduced by the distance the pilot requires to react to an approaching obstacle x_τ and the distance that is needed to attain the maximum climb angle $x_{maneuver}$. Note that x_τ is calculated by multiplying the pilot reaction time τ_p with the current forward speed V [Eq. (2)]. Also, τ_p is assumed to be 0.8 s, based on measurements during a reaction-onset experiment performed by Hosman and Stassen [21]. The maneuver distance $x_{maneuver}$ is calculated based on Eq. (3) and is based on the maximum climb path angle change of $\dot{\gamma}_{max} = 5$ deg, which is assumed to be constant:

$$x_\tau = \tau_p \cdot V \qquad (2)$$

$$x_{maneuver} = \frac{V}{\dot{\gamma}_{max}} \cdot \left(\frac{1}{\sin(\gamma_{max})} - \frac{\cos(\gamma_{max})}{\sin(\gamma_{max})} \right) \qquad (3)$$

The maximum effective climb angle γ_{limit} can now be calculated via Eq. (4). Note that γ_{limit} depends on the current forward speed through a change in γ_{max}. If the forward speed decreases, γ_{max} generally increases up to a maximum of 90 deg at zero forward speed, signifying the capability to increase altitude while hovering. Therefore, γ_{limit} is the maneuver limitation at the current forward speed, which is not necessarily the scenario target speed of 60 kt:

$$\tan(\gamma_{limit}) = \tan(\gamma_{max}) \left(1 - \frac{x_\tau + x_{maneuver}}{d_0} \right) \qquad (4)$$

C. Advisory Display
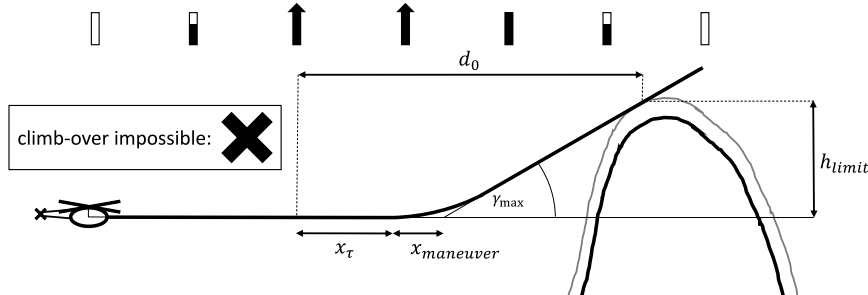
Knowing the calculated maximum effective climb angle γ_{limit}, an advisory display is developed. The advisory symbol warns the pilot about an approaching obstacle, and it will provide a discrete suggestion of when to initiate a pull-up maneuver. The principle design of the advisory symbol is inspired by a study conducted by Kahana [9] (Fig. 4). The depicted empty bar at the first position is always shown to the pilot. When an obstacle approaches, the bar gradually fills up until it gives the discrete suggestion to initiate a flight-path angle change. Passing over the obstacle's edge will cause the bar to gradually empty again. If the pilot does not initiate the climbing maneuver in time, and a climb-over is no longer possible at the given forward speed and the given pilot and model delay constraints, the symbol will change to an X, indicating that a forward speed reduction is necessary to avoid a collision.

The fullness of the symbol is calculated based on the maximum effective climb angle γ_{limit} and the vertical angle between the helicopter and the position of the upper tip of the approaching obstacle's safety zone (10 ft above the obstacle's tip; see Fig. 5). As an obstacle approaches, this angle $\gamma_{obstacle}$ between the horizontal plane and the obstacle's safety zone's tip increases. The advisory symbol starts filling up as the difference between $\gamma_{obstacle}$ and the effective maximum flight-path angle γ_{limit} is reduced to 3 deg. At a 1 deg difference, the arrowhead starts showing. If the angle of the safety zone's top is more than 1 deg larger than the maximum effective climb angle, the X symbol appears, indicating "climb-over impossible." The angle limits have been chosen iteratively to provide a reasonable arrow fill-up speed, based on the target velocity, target altitude, and obstacle height in this experiment.

D. Constraint-Based Display

The constraint-based display directly shows the maximum effective climb angle γ_{limit} to the pilot via a HUD symbol. It does not incorporate any terrain or obstacle data but relies on the pilot to connect the visual information of γ_{limit} and the approaching obstacle to decide when to initiate a climb-over or when to reduce forward

Fig. 4 Advisory symbology for the climb-over maneuver, inspired by Ref. [9].

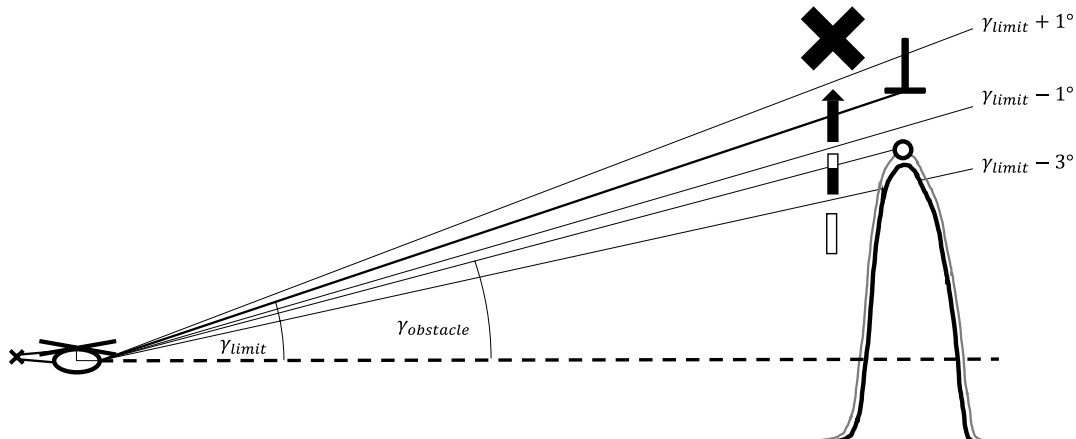

Fig. 5 Relationship between γ_{limit}, $\gamma_{obstacle}$, and the different phases of the advisory display. Advisory symbol depends on $\gamma_{obstacle}$: as obstacle protrudes higher and higher into flight path, advisory changes from empty arrow box to filled arrow, to the climb-over impossible cross.
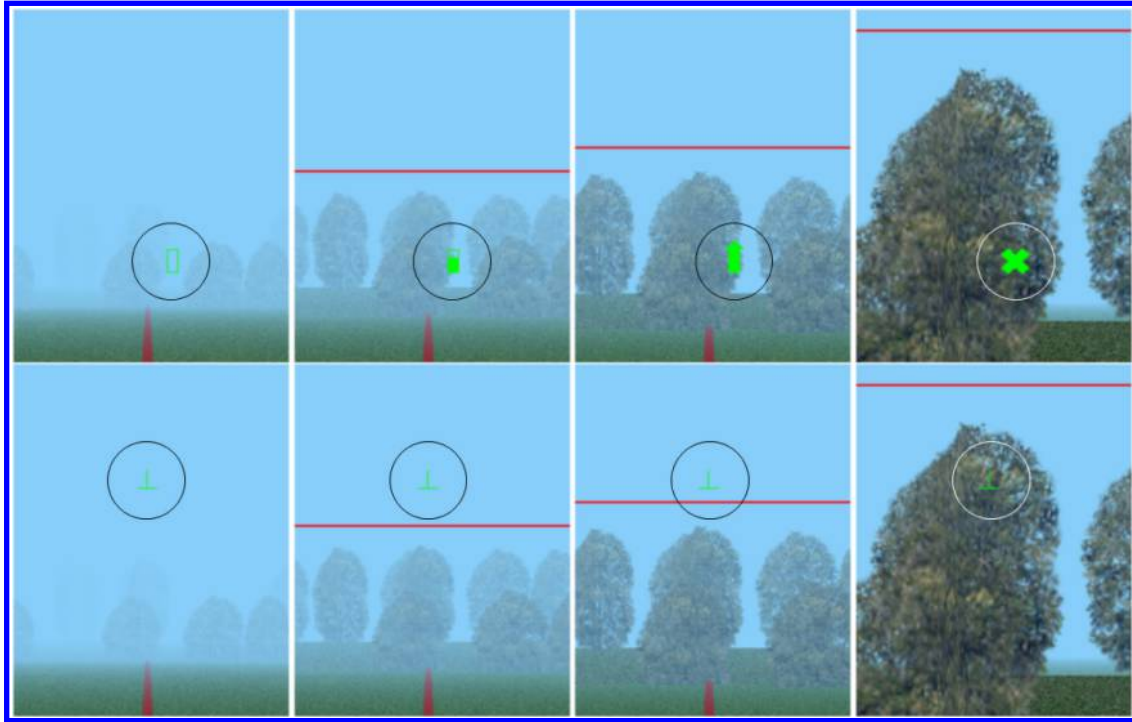
Fig. 6 Advisory (top) and constraint-based display variants (bottom) while approaching an obstacle.

speed to avoid a collision. When a climb-over is impossible with the current forward speed (indicated by γ_{limit} being displayed in front of the obstacle, and not above it), it requires the pilot to recognize this and react accordingly by reducing speed. Figure 5 summarizes the appearance of the two display variants, based on the maximum effective climb angle γ_{limit} and the angle between the horizontal and the obstacle's safety zone's tip. Figure 6 shows the two display variants as they appear on the HUD during an approach with 60 kt, at distances of (from left to right) 300, 200, 150, and 100 m to the obstacle. In this image, the contrast between the symbol and the sky is rather poor. In the simulator, contrast was more pronounced and the symbology was always easily visible. The circle in each picture only serves to highlight the relevant symbol, it is not part of the implemented HUD.

E. Display Categorization

To relate this paper's displays to other helicopter display types, a diagram to categorize helicopter display systems of Minor et al. is reproduced in Table 2 [8]. First, they distinguish between helmet-mounted (head-up) displays and panel-mounted (head-down) displays. Second, they differentiate between what kind of information is shown to the pilot: either the display mainly shows primary pilotage information (e.g., altitude, attitude, airspeed, position, and environmental parameters) or the display provides guidance cues (e.g., an optimal target maneuver trajectory). This paper's displays fall into categories I and IV, as well as into the space between the two categories. The employed baseline HUD and the included obstacle detection and contour drawing system fall into category I. The advisory symbol for obstacle avoidance falls into category IV. Lastly,

the constraint-based steepest climb indication display is located somewhere between categories I and IV because it provides more information to the pilot than just primary pilotage information, but it does not provide a direct or discrete maneuver cue, giving the pilots more freedom in how to react to the approaching obstacle. Based on the provided information, the pilots need to decide themselves when to initiate the pull-up maneuver.

III. Methodology

A. Apparatus

The experiment took place in the SIMONA research simulator at Delft University of Technology [22], which is depicted in Fig. 7. The cockpit window setup resembled a fixed-wing airline cockpit with a field of view of 180 by 40 deg; the typical chin-window view of helicopters was obstructed. The outside visual was collimated, optically appearing at or near infinity to the pilots. The HUD symbology was projected on top of the outside view in the center of view, and no helmet-mounted technology was used. Care was being exercised that all symbology was visible during all typical pitch angles during the anticipated maneuvers, even with the limited viewing area. The simulator contained a collective lever, a cyclic stick, and pedals. During the experiment, the simulator cabin door was closed and the light was turned off. The used model was an analytical model

Table 2   Categories of display systems to support helicopter control, reproduced from the work of Minor et al. [8]

	Displayed image primary pilotage	Guidance algorithm primary pilotage
Helmet-mounted display	Category I: Reliable option with 1:1 magnification	Category IV: Focusing on two-dimensional cues through three-dimensional picture can be difficult; permits coupling flight controls
Panel-mounted display	Category II: Unusable	Category III: Excellent option for following guidance; permits coupling flight controls

Fig. 7   SIMONA research simulator.

Table 3 Pilot participant demographic data (CPL denotes commercial pilot license)

Group	Number	Flight hours Average	Standard deviation	Type of license (amount) PPL	CPL	Other
All pilots	12	1906	2326	5	6	1
3000 and more flight hours	4	5025	1246	0	3	1
1000 and less flight hours	8	346	207	5	3	0

of a Messerschmitt–Bölkow–Blohm Bo105 helicopter [23]. The motion system of the simulator was deactivated. Adding motion would improve the realism of the simulation, but it could confound the experiment because it could distract pilots from the employed visual systems. This would make it more difficult to analyze and isolate the impact of the visual augmentations on the data.

B. Participants

Twelve helicopter pilots with varying experience [minimum private pilot license (PPL); 100 flight hours] participated in this experiment. Table 3 shows some participant demographic aggregates. The participating pilots can be categorized into two distinct groups: one group of eight pilots with less than 800 flight hours, and one group of four pilots with more than 3000 flight hours.

C. Task

The scenario emulated a low-altitude helicopter surveillance task to inspect oil pipelines for leakages. To quickly find the leakage, a flyover at a low altitude of 30 ft and a speed of 60 kt had to be conducted. At intervals between 500 and 900 m, the pipeline was covered by a rising ground slope, and a tree line with a height of 80 ft obstructed the optimal flight path. Six different obstacle courses with varying distances between obstacles were defined, as shown in Table 4. The first obstacle always appeared after 700 m, and the following distances varied per experiment course. The obstacle courses were rotated throughout the experiment per run in a balanced order. Figure 8 shows a conceptual view of the obstacle course.

Real-world pipeline inspection tasks are not performed at this altitude–speed combination but typically at a higher altitude as well as a higher speed. By pairing 30 ft with 60 kt, the task in this paper is purposefully made more difficult to control. This increase in difficulty aims to provoke more different responses and pilot preferences based on the employed displays. If the task would have been very easy to perform with very good performance ratings in every condition, the performance and pilot workload differences between different displays were expected to decrease. It is important to note that this artificial increase of difficulty diminishes the task's likeness to real-world applications.

The instruction given to the pilots was the following:

The first priority is to avoid collision with any obstacle or the ground, maintaining a separation of at least 10 ft. The second priority is to maintain a forward speed of 60 knots, stay centered above the pipeline, and maintain an altitude of 30 ft, smoothly climbing over any obstacles that block your optimal flight path. After climbing over an obstacle, please try to attain the target altitude again as soon as possible.

One experiment run consisted of an obstacle course with the length of 4700 m, which contained six obstacles at semirandom locations. After every experiment run of approximately 3 min, two performance scores were communicated to the pilots: the root-mean-square tracking error of the forward speed, and the root-mean-square tracking error of the target altitude. Naturally, the altitude tracking error could never reach zero because climbing over an obstacle required a deviation from the target altitude. In addition, the minimum vertical clearance and the average vertical clearance above the obstacles were communicated to the pilots. The pilots could therefore aim to improve their scores and safety clearances between runs.

D. Independent Variables

The independent variables of this experiment are *display* and *visibility*. A third independent variable of *(off-)nominal situation*, which introduces off-nominal situations in a small percentage of runs per experiment condition, is introduced in the following paragraph. The display conditions are 1) baseline HUD, 2) baseline HUD + advisory display, and 3) baseline HUD + constraint-based display.

Table 4 Distances between obstacles of the six defined obstacle courses

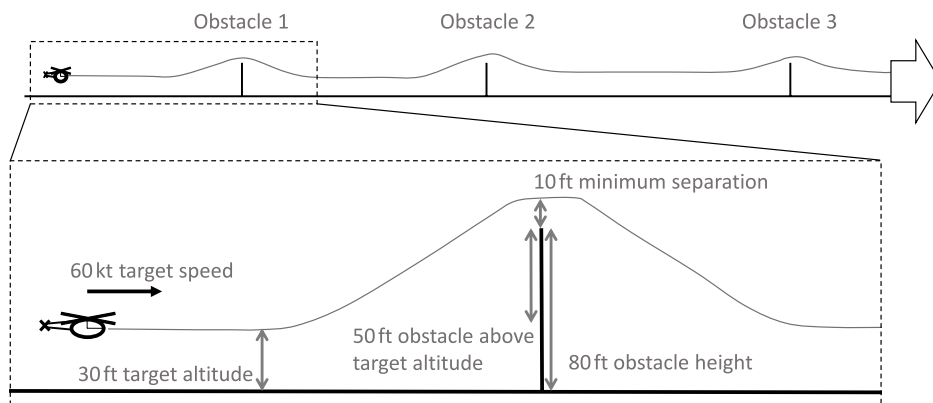| Course no.	Obstacle 1, m	Obstacle 2, m	Obstacle 3, m	Obstacle 4, m	Obstacle 5, m	Obstacle 6, m
1	700	750	600	750	600	900
2	700	650	800	650	800	500
3	700	600	850	650	650	850
4	700	800	650	650	650	650
5	700	650	750	750	550	900
6	700	750	650	650	850	500

Fig. 8 Principle obstacle course design.

Table 5　Experiment independent variables and resulting experiment conditions A–F

Experiment conditions	Visibility	
	High	Low
Baseline HUD	A	B
Baseline HUD + advisory display	C	D
Baseline HUD + constraint-based display	E	F

The baseline HUD condition conceptually emulates current helicopter HUD systems like the one employed by Münsterer et al. [6], including visual obstacle highlighting but excluding any maneuver cues or other support tools. In this setup, the additional value of the employed obstacle avoidance support systems, compared to a state-of-the-art baseline system, can be analyzed. The visibility was set to 300 m in the high condition and to 200 m in the low condition. The order of experiment conditions was balanced between pilots. Each experiment condition was flown five times per pilot, including one nonrecorded warmup run. Table 5 summarizes the independent variables and experiment conditions.

To investigate the effect of off-nominal situations, failure events were deliberately inserted into some experiment runs, creating the third independent variable of (off-)nominal situation (nominal, off-nominal) for performance and safety measures, as described in Sec. III.E. Some obstacles were recognized later than usual by the obstacle detection and contour drawing system (which is part of the baseline HUD) at a distance of 50 m instead of 300 m. The dependent measurements while approaching and reacting to unexpected events are cut from the remaining experiment data and analyzed separately. The pilots were briefed on the possible occurrence of failures like this, and they encountered one such off-nominal event during their training and acclimatization phase.

Table 6 summarizes the detection distances of the outside visuals as well as the obstacle detection and contour drawing system per experiment condition. Assuming a perfect approach at 60 kt and 30 ft, it takes 3.9 s between the time when the obstacle contour first appears at a distance of 300 m and when the maximum effective climb angle of $\gamma_{\text{limit}} = 5.82$ deg coincides with the red warning contour around the obstacle. The pilots have this time to register the appearance of the obstacle and initiate the climb-over maneuver at the distance and aggressiveness of their choosing.

During low-visibility and off-nominal situations, the obstacle only appears visually at a distance of 200 m. The obstacle contour warning only appears at a distance of 50 m, making it deliberately unusable for a timely pull-up control action. At this point, again assuming a perfect approach, the tip of the obstacle (including the 10 ft minimum distance) appears at a 5.22 deg angle, which is very close to $\gamma_{\text{limit}} = 5.82$ deg. To still clear the obstacle, the pilots have to react within 0.7 s, reduce their forward speed, or exceed the limits prescribed to the constraint calculation (reacting quicker than in 0.8 s, exceeding a 5 deg /s flight-path angle rate, and/or using more than 80% of the available power).

These events, which require pilot actions very close to (or even outside of) the prescribed display limits and suggestions, enable the analysis of the robustness of the pilot–vehicle system toward system malfunction. Each condition contained four off-nominal situations, with one experiment run containing, at most, two off-nominal situations.

Table 6　Visibility and obstacle detection distances, dependent on visibility condition and unexpected events

Conditions	Visibility condition	Viewing distance, m	Unexpected events	Obstacle detection distance, m
A, C, E	High	300	Yes	300
A, C, E	High	300	No	50
B, D, F	Low	200	Yes	300
B, D, F	Low	200	No	50

E.　Dependent Measures

The dependent variables are *performance*, measured via the deviation [root-mean-square-error (RMSE)] from the ideal target altitude, lateral position, and speed (i.e., clearing an obstacle always causes an altitude deviation from the ideal altitude); *safety*, measured via the vertical clearance of the climb-over maneuvers over obstacles, as well as the number of intrusions into the minimum clearance zone or the obstacle itself; *workload*, measured via the subjective rating scale mental effort (RSME), and given to the pilots after each condition (developed by Zijlstra and Van Doorn [24], as cited in Ref. [25]); and *situation awareness*, measured via the subjective scale situation awareness rating technique (SART) [26], likewise given to the pilot after each experiment condition.

Although this task seems suitable to be used in a handling qualities analysis, the chosen performance metrics are deliberately defined in a simpler matter, without specifying desired or adequate boundaries. This is done in order to simplify the evaluation of the flown trajectories by the participating pilots. The employed questionnaires are dependent on neither preexisting knowledge about handling qualities rating from the pilots nor on the participants forming a consistent understanding about adequate and desired performance boundaries.

Control strategy is analyzed by calculating the average control activity, the trajectory spread, the velocity at maximum altitude, the pull-up initiation location, and the characteristic maneuver parameters of fitted maneuvers based on gap-closing τ theory as described by Padfield [27].

The workload and situation awareness ratings were collected per condition, not differentiating between nominal and off-nominal situations. Performance, safety, and control strategy metrics are calculated for nominal and off-nominal situations separately. After all conditions, the pilots were asked to complete a questionnaire about the whole experiment, covering their preferences between the different display systems in nominal and off-nominal situations. In the Appendix, Figs. A1–A3 depict the employed questionnaires.

F.　Control Variables

Control variables comprise the simulator setup; task; target speed and altitude; the used six-degree-of-freedom helicopter model; and the baseline HUD with altimeter, speed tape, flight-path vector, and obstacle detection and contour drawing system, as described in Sec. II.

G.　Data Processing

Workload and situation awareness ratings are collected once per experiment condition and pilot. They are normalized to a mean of zero and a standard deviation of one (Z-scored) per participant to account for subjective scaling and offset differences. Performance, safety, and control strategy results are averaged per experiment participant and condition, resulting in one data point per participant per experiment condition.

Anderson–Darling tests for normality of data are performed per experiment condition (separately for nominal and off-nominal cases when possible), resulting in 12 test outcomes per dependent measure. If the null hypothesis ("data are drawn from a normal distribution") is rejected in more than 3 out of 12 cases at $\alpha = 0.05$, nonparametric two-way Friedman tests are employed to analyze the data. In this case, the independent variables display and visibility are combined into one independent variable with six-degree-of-freedom *display* × *visibility*. Otherwise, a parametric three-way analysis of variance (ANOVA) is used.

The preceding methodology analyzes both nominal and off-nominal situations in one combined test statistic. However, due to the difference in the number of data points per pilot between nominal (twenty) and off-nominal (four) situations, nominal and off-nominal situations are afterward analyzed separately as well. To account for multiple tests, a Bonferroni correction with a significance value of α is carried out per dependent measure: the first statistic test, comparing all data, is carried out at $\alpha = 0.03$; and the following tests for separate nominal and off-nominal situations are carried out at $\alpha = 0.01$,

resulting in an overall significance value of $\alpha = 0.03 + 0.01 + 0.01 = 0.05$ for every dependent measure.

To analyze the maneuver strategies of the pilots in more detail, the complete trajectory is divided into three parts: *pull-up*, at a distance between 320 and 50 m to the obstacle while approaching the obstacle; *flyover*, at ± 50 m around the obstacle; and *descent*, between 50 and 180 m behind the obstacle.

In case of workload and situation awareness, no separate data points for nominal and off-nominal situations exist, which results in six test outcomes per dependent measure. If normality is rejected in more than two cases, nonparametric two-way Friedman tests are used. Otherwise, a two-way ANOVA is used.

H. Hypotheses

Performance increases when using any of the support displays in nominal situations because both displays provide more information to the pilot, enabling him or her to more consistently follow his or her preferred flyover trajectory. The effect is stronger for the advisory system because it requires less cognitive resources from the pilot, and it is easier to follow its advice. In off-nominal situations, only the constraint-based display improves performance, when compared to the baseline HUD.

Workload decreases when using any of the support displays because both provide additional information to the pilot that supports him or her in performing the task. The effect is stronger with the advisory display because it provides easy-to-follow maneuver advice compared to the constraint-based display, which requires more cognitive resources from the pilot.

Situation awareness increases when using any of the support displays because the pilot receives more information about his current aircraft state and its relation to the outside world (obstacles). This effect is expected to be stronger with the constraint-based display because it enables the pilot to perceive the internal maneuver limitations of the helicopter (in the form of the maximum effective climb angle γ_{limit}) and connect these to the external limitations of the approaching obstacle.

Safety is expected to behave differently between its measurement techniques. In nominal situations, the minimum clearance above obstacles decreases when using any of the support displays. As the pilot is made aware of the maneuver limitations by both support displays, the pilot might decide to reduce the safety margin (while still staying above the minimum clearance above obstacles) to increase performance. However, the percentage of unsafe clearances lower than 10 ft will decrease when using any of the support displays because both displays can support the pilot in detecting and reacting to an approaching obstacle. In off-nominal situations, the percentage of unsafe clearances decreases when using the constraint-based display, and it increases when using the advisory display, as compared to the baseline HUD condition. The advisory display might give a false

sense of security in off-nominal situations, causing a later reaction to the obstacles than when using the baseline HUD. In contrast, the constraint-based display still provides the pilot with information about his or her maneuver capability, as well as its relation to outside obstacles.

Concerning control strategy, a decrease in visibility and off-nominal situations causes a later pull-up initiation. The advisory display causes a decrease of maneuver variability, and the flown maneuvers will group closely around the suggested maneuver. The constraint-based display will cause a broader spread of flown maneuvers while also enabling pilots to fly closer to the edge of possible maneuvers, i.e., later pull-up. The constraint-based display gives the pilots the freedom to choose for themselves at what distance to the maneuver limit they initiate the pull-up maneuver.

A reduction of visibility increases workload, decreases situation awareness, reduces performance, and leads to later pull-up initiations and more flyovers at unsafe clearances. The aforementioned hypothesized effects of displays and off-nominal situations are amplified in low-visibility conditions.

IV. Results

Figure 9 shows results of two conditions: nominal high-visibility flyovers with the basic HUD, and off-nominal low-visibility flyovers with the advisory display. At a first glance, the flown trajectories differ in spread as well as pull-up location. The following subsections will elaborate on the effects of different display, visibility, and (off-) nominal situations on all dependent measures.

Analyzing the dependent measures did not reveal observable differences between repeating runs of the same condition; there is no pronounced learning effect within the recorded experiment runs. The training phase seems to have been sufficient to acclimatize the pilots with the experiment. An analysis of learning effects per dependent measure is therefore omitted.

A. Workload

Figure 10 shows box plots of Z-scored RSME measures per experiment condition. Normality is not rejected for any condition; therefore, two-way ANOVA test statistics are used. Workload seems to differ between the employed displays, especially in high visibility. However, there is no significant effect: $F_{(2, 66)} = 2.41$, $p = 0.10$. In good visibility, there is a trend of decreasing workload when switching from the baseline HUD to the advisory display, as well as of further decrease in workload when switching to the constraint-based display. In bad visibility, however, the median actually slightly increases with the advisory display as compared to the baseline HUD. Low visibility significantly increases workload [$F_{(1, 66)} = 13.60$, $p < 0.001$], which is in line with the expected effect of worsening visibility.
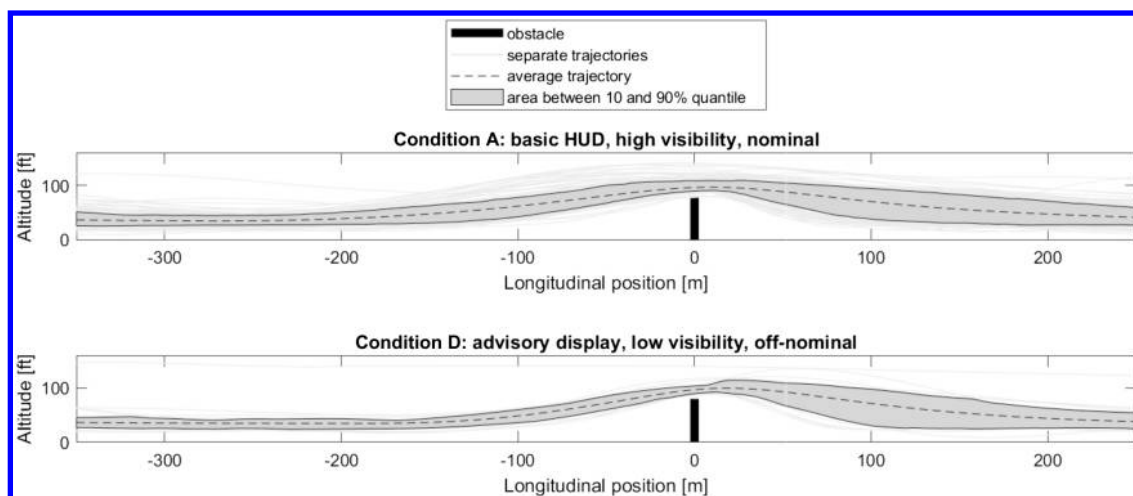

Fig. 9   Flown trajectories in nominal cases in condition A and off-nominal cases in condition D.
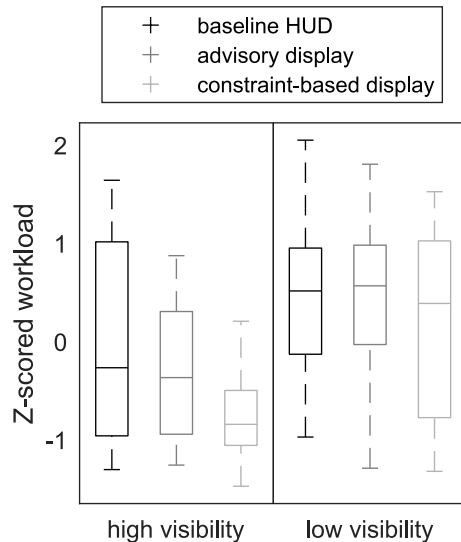
Fig. 10   Workload questionnaire results per experiment condition: Z-scored per participant. Large Z-scored workload values correspond with large reported workload measures, and vice versa.

B.   Situation Awareness

Normality is rejected in one out of six conditions, and two-way ANOVA test statistics are used. Z-scored SART measures, as shown in Fig. 11, are not significantly affected by display [$F(2, 66) = 1.18$, $p = 0.31$]. Considering the median values per condition, there is a trend of increasing situation awareness when switching from the baseline HUD to the advisory display; and there is a further increase when switching to the constraint-based display. Just as with workload, the median of the advisory display in bad visibility does not follow this trend, and it is actually lower than the medians of the baseline HUD and the constraint-based display. Lower visibility significantly decreases situation awareness [$F(1, 66) = 9.72$, $p < 0.01$], as expected.

C.   Performance

The average altitude, speed, and lateral deviation are discussed in parallel. Figure 12 shows box plots of the altitude deviation per experiment condition, Fig. 13 shows box plots of the airspeed deviation, and Fig. 14 shows box plots of the lateral position deviation.
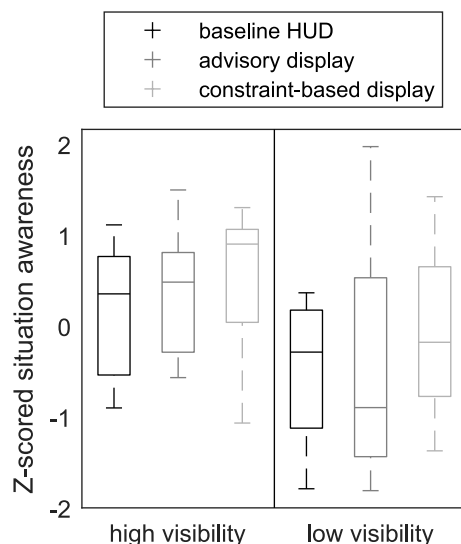

Fig. 11   Situation awareness questionnaire results per experiment condition: Z-scored per participant. Large Z-scored situation awareness values correspond with large reported situation awareness measures, and vice versa.

Normality is rejected in 4/12 (altitude), 0/12 (speed), and 6/12 (lateral) cases. Speed is analyzed using parametric tests, altitude and lateral performance are analyzed using nonparametric tests. No significant effect on average altitude or lateral deviation of (off-) nominal situation or (display × visibility) is revealed, and $p > 0.03$ in all cases. Likewise, there is no significant effect of display, visibility, or (off-)nominal situation on speed: $p > 0.03$. There is one trend visible: off-nominal situations increase the speed deviation compared to nominal situations [$F(1, 134) = 2.53$, $p = 0.11$]. This could be explained by a change in control strategy in off-nominal situations, focusing less on maintaining forward speed but prioritizing the more important goal ("do not collide with obstacle").

Analyzing only nominal situations reveals a significant effect of visibility on altitude deviation [$\chi^2(1, 66) = 7.99$, $p < 0.01$] and lateral deviation [$\chi^2(1, 66) = 7.61$, $p < 0.01$], and lower visibility leads to less deviation in both measures. In off-nominal situations, no significant effects can be observed, and $p > 0.01$ in all cases.

Analyzing altitude, speed, and lateral deviation in the separate maneuver stages reveals that only altitude deviation during the pull-up maneuver part is significantly affected by any of the experiment independent variables. There is also a trend visible in the effect on speed deviation during descent. Both effects are discussed in the following.

Figure 15 shows the altitude deviation during pull-up. Normality is rejected in 7/12 cases, and the used two-way Friedman test reveals a significant effect of (off-)nominal situation [$\chi^2(1, 132) = 15.49$, $p < 0.001$] as well as of the combined display × visibility variable [$\chi^2(5, 132) = 19.98$, $p < 0.03$].

Testing the nominal and off-nominal pull-up datasets separately, however, reveals that the effect of the combined display × visibility variable is caused solely by visibility. In nominal situations, bad visibility significantly decreases altitude deviation [$\chi^2(1, 66) = 7.61$, $p < 0.01$]. In off-nominal situations, the effect is even stronger [$\chi^2(1, 66) = 39.24$, $p < 0.001$]. This can be explained by the reduced distance at which the obstacle becomes visible, as explained in Table 6. In good visibility, the obstacle becomes clearly visible at a distance of 300 m, irrespective of nominal or off-nominal situations, which may in turn prompt the pilots to initiate an altitude change. In bad visibility and nominal situations, only the contour of the obstacle becomes visible at 300 m; the obstacle itself only becomes visible 100 m later. The appearance of only the contour line represents a less intense stimulus than the appearance of a whole line of trees directly in the current flight path. This reduction of visual stimulus and delayed visual appearance of the actual obstacle likely caused a delay in pull-up control action, leading to a smaller altitude deviation during the pull-up trajectory stage. In bad visibility and off-nominal situations, the obstacle only becomes noticeable at a distance of 200 m. The pull-up control action is delayed even further, explaining the highly significant effect of visibility in off-nominal situations.

Speed deviation during the descent trajectory is shown in Fig. 16. There is a trend of increasing speed deviation during descent when encountering off-nominal events: $F(1, 134) = 3.69$, $p = 0.06$. Even though the speed deviation was not significantly different between conditions during pull-up and flyover, it seems like off-nominal events cause a greater speed deviation while "recovering" from an unexpected avoidance maneuver, and not during the maneuver itself.

D.   Safety

Figure 17 shows box plots of the averaged safety clearances. Normality is rejected in 6/12 cases, and nonparametric Friedman tests are used. No significant effects can be observed, and $p > 0.03$ for every independent variable. It can be observed that in bad visibility, the advisory display is the only condition whose data protrude visibly into the unsafe clearance area less than 10 ft. However, this is caused by the data of only two pilots: one pilot consistently undershot the safety clearance in this condition, and the other pilot generally cleared the obstacle while generating two extreme outliers with negative clearance values. In other conditions, both pilots generally cleared the obstacles with sufficient clearance. The pilot who consistently undershot the clearance has one of the lowest flight hour
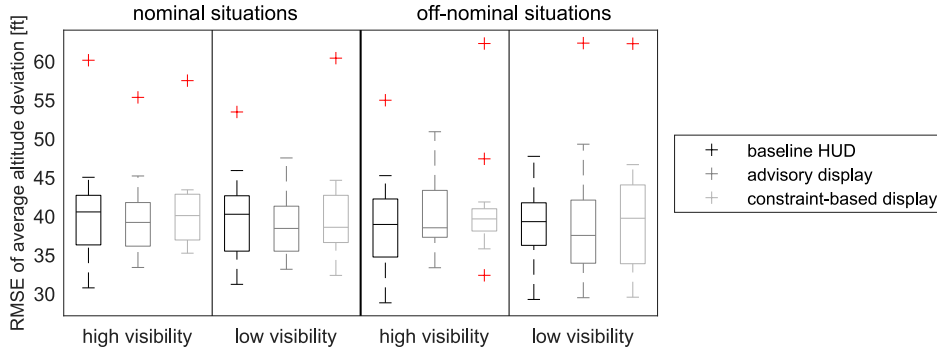
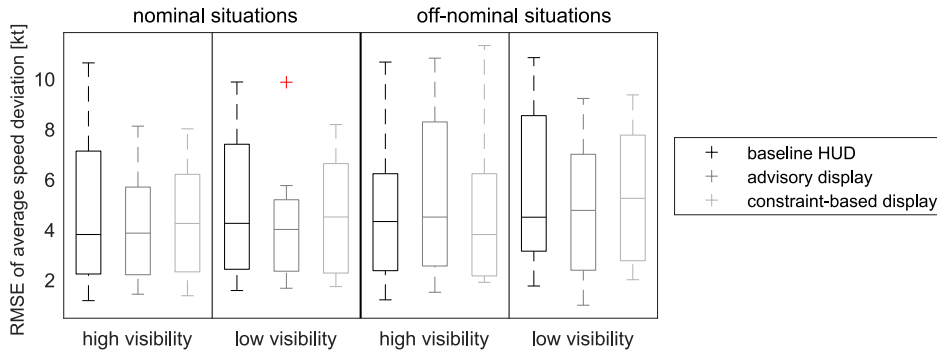**Fig. 12   Box plots of average altitude deviation per visibility, display, and situation.**

Fig. 13   Box plots of average speed deviation per visibility, display, and situation.
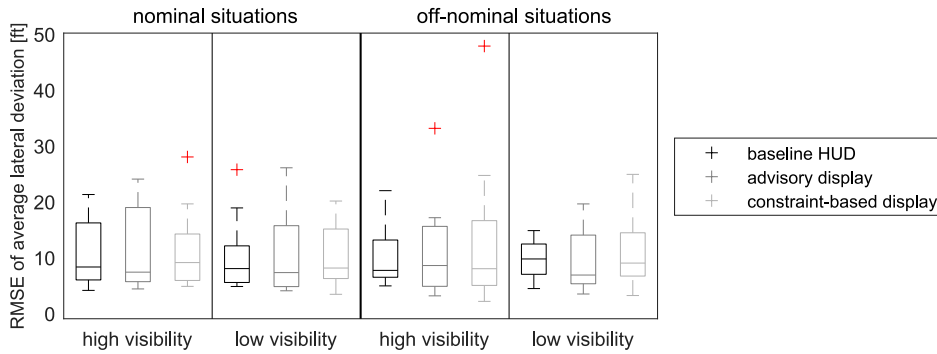

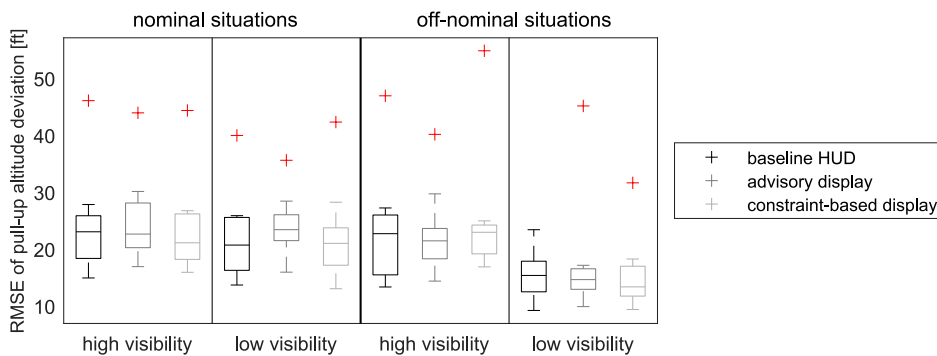**Fig. 14   Box plots of average lateral deviation per visibility, display, and situation.**

Fig. 15   Box plots of altitude deviation during pull-up per visibility, display, and situation.

values of the participants, which might explain his/her trouble in clearing the obstacle. However, chronologically, this condition was his/her fourth condition; and he/she completed all previous conditions without entering the unsafe clearance area so often. Because this behavior only occurred in this condition, and is only visible in this specific dependent measure, the protrusions of these two pilots into negative clearances are treated as outliers and cannot be generalized to a larger pilot population.

In off-nominal situations, the average and median safety clearances slightly increase when switching from the baseline HUD to the
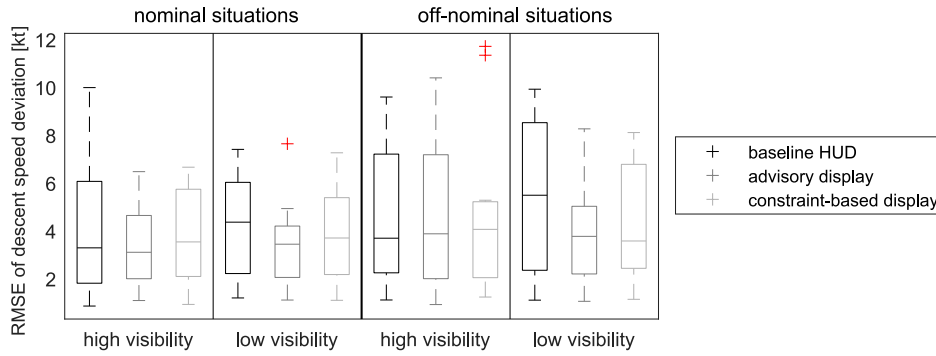
Fig. 16   Box plots of speed deviation during descent per visibility, display, and situation.
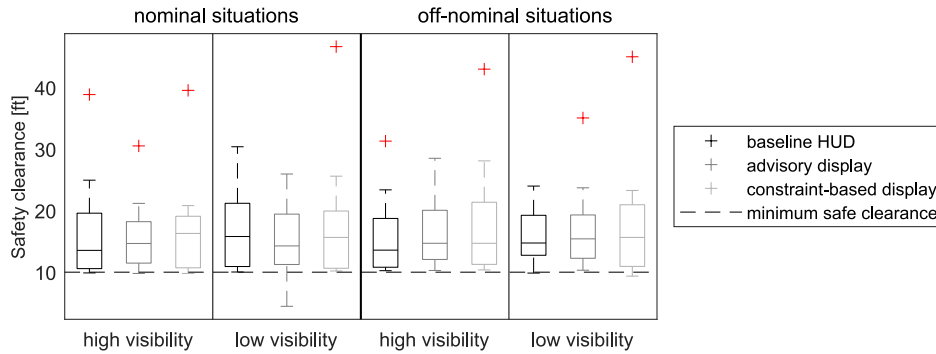

Fig. 17   Box plots of average safety clearances per experiment condition, in nominal and off-nominal situations.

advisory display, and they increase further when switching to the constraint-based display. Analyzing nominal and off-nominal situations separately reveals no significant effects, but trends of decreasing safety clearance when switching from high visibility to low visibility [nominal: $\chi^2(1, 66) = 6.52$, $p = 0.011$; and off-nominal: $\chi^2(1, 66) = 5.84$, $p = 0.016$].

The relative amount of unsafe clearances less than 10 ft with respect to the total number of climb-over maneuvers is shown in Fig. 18. In nominal situations, visibility does not seem to influence the percentage of unsafe clearances. In off-nominal situations, using the baseline HUD leads to the highest percentage of unsafe clearances (17 and 19%, respectively).

Off-nominal situations consistently increase the percentage of unsafe clearances, except when using the constraint-based display in good visibility or the advisory display in low visibility. In high visibility, using the constraint-based display leads to the lowest number of unsafe clearances, given an off-nominal situation was encountered (8%). In low visibility, the advisory display causes the least unsafe clearances (10%). In general, using the advisory or the constraint-based displays seems to increase the resilience toward unexpected events as compared to the baseline HUD. The constraint-based display causes the least amount of unsafe clearances in three out of four conditions.

E.   Pull-Up Initiation

To determine the time of maneuver initiation, a method of Scaramuzzino et al. [28] is used. This method calculates the maneuver initiation time based only on the control input data. It identifies the monotonously increasing control input section with the highest root-mean-square deviation from its starting point, in the direction of the expected maneuver: an increase in collective and/or a pitch-up cyclic input. After identifying the strongest control input section, the starting time of this section is defined as the maneuver onset.

This algorithm is applied to every obstacle approach trajectory. The data are limited to the probable location of pull-up initiation, between 320 and 100 m in front of the obstacle. If both collective and cyclic pull-up initiation times are determined, the control action with the higher intensity is chosen. Control intensity is measured through the root-mean-square deviation from the maneuver starting position, scaled to a percentage of the respective maximum stick deflection. Figure 19 shows an example trajectory, including longitudinal and collective control inputs and the largest identified control actions.

The calculated pull-up initiation locations, averaged per condition, are shown in Fig. 20. There is a significant effect of visibility on pull-up location $F(1, 134) = 17.66$, $p < 0.001$, as well as a significant effect of (off-)nominal situation $F(1, 134) = 17.56$, $p < 0.001$. There is also a significant interaction effect between visibility and
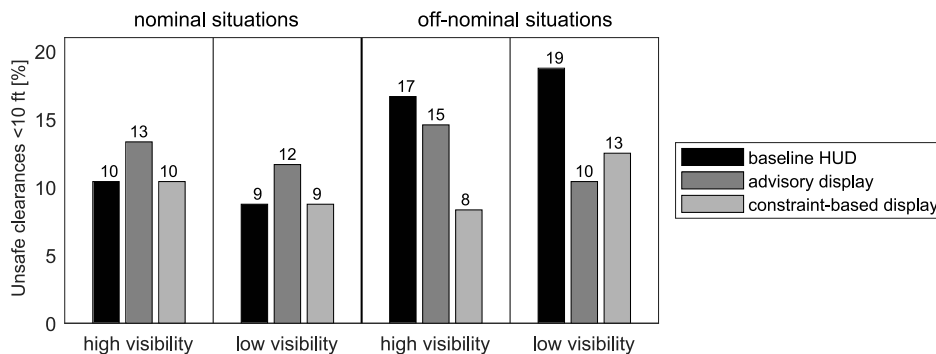

Fig. 18   Percentage of unsafe clearances per experiment condition, in nominal and off-nominal situations.
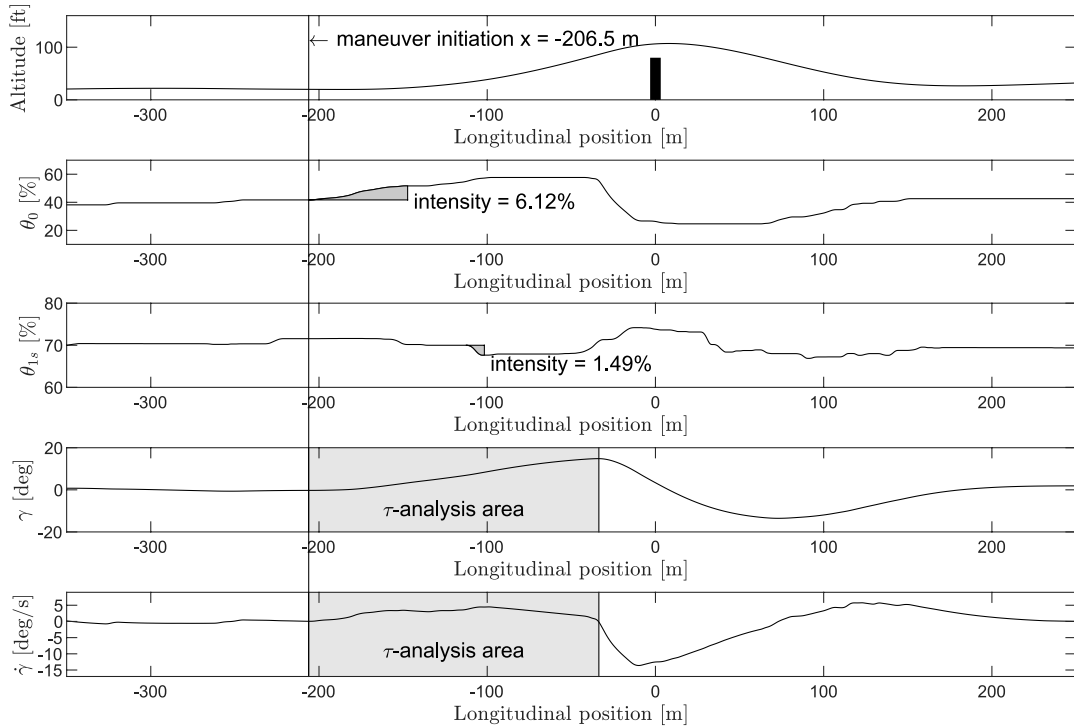
Fig. 19 Example flyover trajectory in good visibility, with the basic HUD, in a nominal situation.
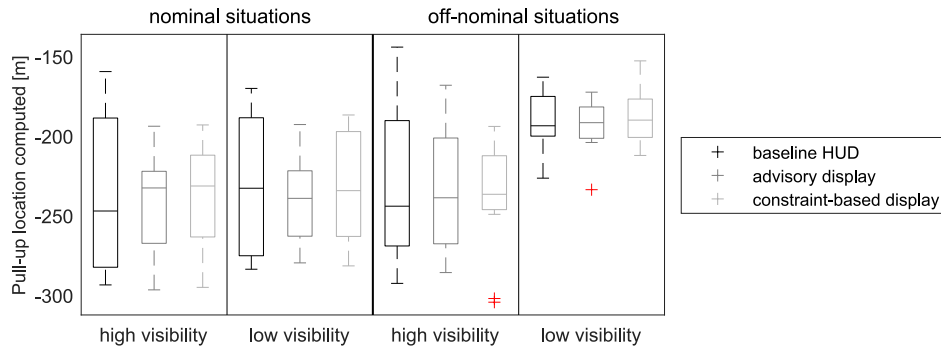

Fig. 20 Box plots of pull-up maneuver onset location per visibility, display, and situation.

(off-)nominal situation $F(1, 134) = 11.65$, $p < 0.001$. When analyzing nominal and off-nominal situations separately, it becomes apparent that visibility only affects pull-up location in off-nominal situations [$F(1, 66) = 34.31$, $p < 0.001$]; there are no significant effects in nominal situations. This can again be explained by the visibility onset distance of the obstacle, depending on the condition (Table 6); only in low-visibility off-nominal conditions is the obstacle completely undetectable at distances greater than 200 m, resulting in significantly later pull-up initiations. In the other conditions,

either the obstacle itself or its contour is visible from a distance of 300 m.

F. Pull-Up Control Strategy: Cyclic Versus Collective

Figure 21 shows a categorization of control strategies to initiate a pull-up maneuver. It is based on the pull-up initiation location computed in the previous subsection. A pull-up is categorized as "cyclic only" if the algorithm did not detect any collective pull-up
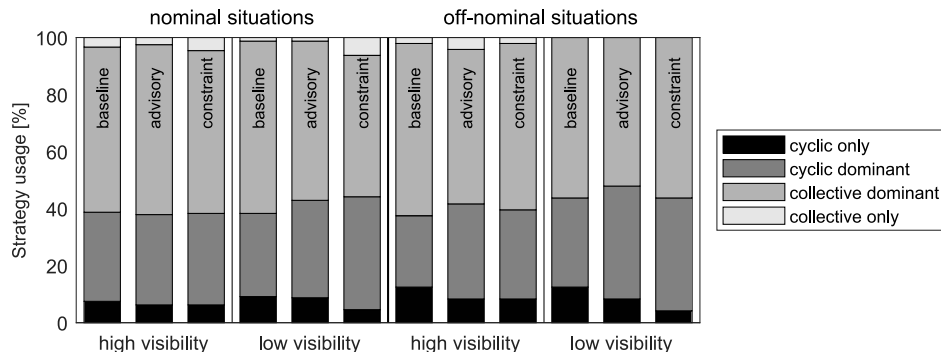

Fig. 21 Control strategy during the pull-up maneuver.

control action in the probable pull-up area. Likewise, it is categorized as "collective only" if no cyclic pull-up control is detected. If both collective and cyclic control actions are identified, the pull-up is categorized as "cyclic dominant" if the cyclic control intensity is greater than the collective control activity (scaled to a percentage of maximum inceptor deflection); otherwise, it is categorized as "collective dominant."

In low visibility, using the constraint-based display leads to a slight decrease in cyclic-only initiations as compared to the other displays. In nominal situations, the constraint-based display seems to elicit more collective-only control actions. In safety-critical off-nominal situations, the constraint-based display leads to the least cyclic-only and collective-only control actions, as well as to an increase of coordinated control approaches. In this dependent measure, no noticeable difference between pilots with less or pilots with more flight experience can be observed in terms of the employed control strategies.

G. Control Activity

For the analysis of the results of this experiment, control activity is defined as the signal power of the control inceptor deflection in a 1 s sliding window. Figures 22 and 23 show box plots of the average cyclic and collective control activity per condition. Normality is

rejected in both cases, and there are no significant effects of (off-) nominal situation or display $\times$ visibility on either collective or cyclic control activity. Analyzing nominal and off-nominal situations separately likewise does not reveal any significant effects. There seems to be an increased spread of cyclic control activity in low-visibility off-nominal situations, possibly caused by the later detection of the obstacle and differing coping strategies per pilot.

While there are no significant differences in average control activity, there might still be differences during the separate maneuver phases, especially pull-up, that could be caused by the smaller obstacle detection distance. Figures 24 and 25 show the collective and cyclic control activities during that maneuver phase. Normality is rejected for both parameters.

There is no significant effect of (off-)nominal situation or display $\times$ visibility on cyclic or collective pull-up control activity. Analyzing nominal and off-nominal situations separately, however, reveals a significant effect of visibility on collective pull-up control activity in nominal situations [$\chi^2(1, 66) = 7.99$, $p < 0.01$]. A decrease of visibility significantly increases collective control in nominal situations. The variability of cyclic control activity seems to increase in off-nominal low-visibility situations, but this is not substantiated by a significant statistical test result.
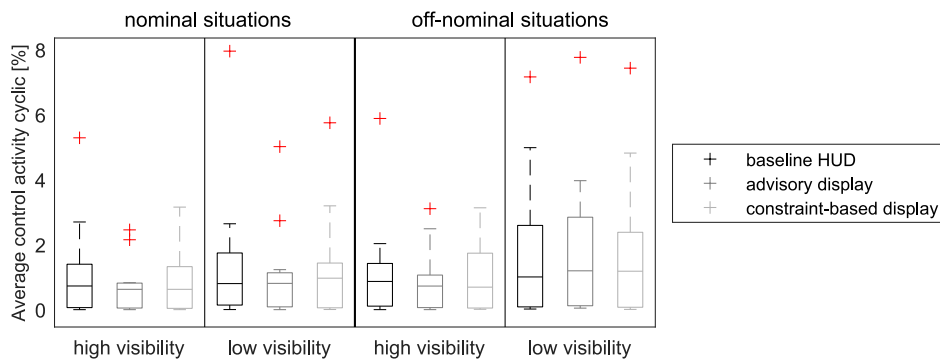

Fig. 22   Box plots of average cyclic control activity per visibility, display, and situation.
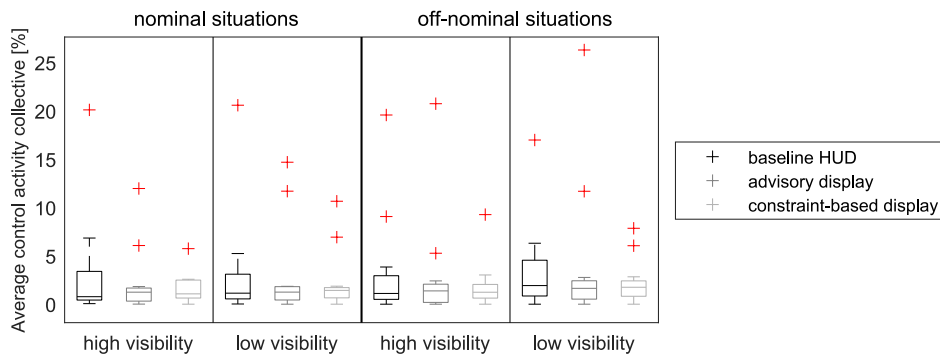

Fig. 23   Box plots of average collective control activity per visibility, display, and situation.
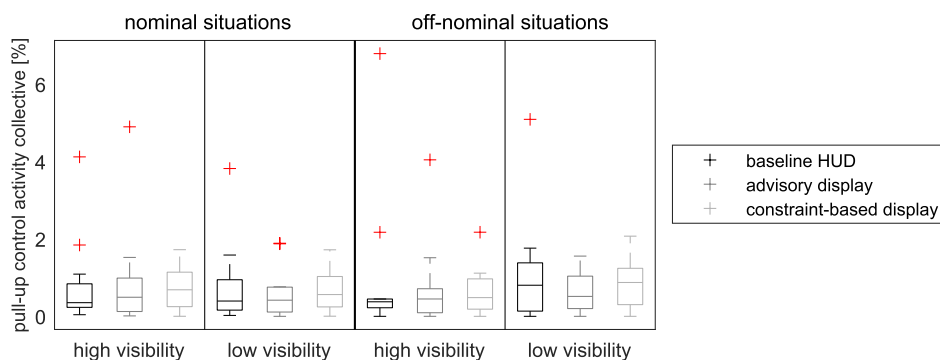

Fig. 24   Box plots of pull-up collective control activity per visibility, display, and situation.
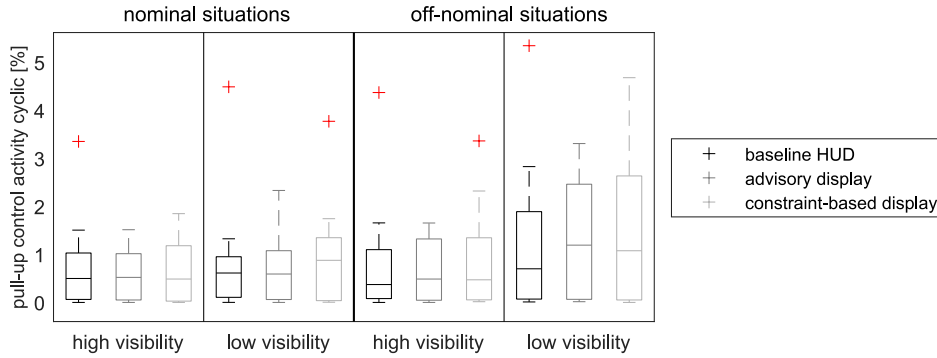
Fig. 25 Box plots of pull-up cyclic control activity per visibility, display, and situation.

H. Trajectory Spread

The average trajectory spread is calculated per pilot as the average root-mean-square difference of the flown altitude trajectories to this pilot's average altitude trajectory in this condition; it is therefore a measure of maneuver variability within one participant. Experiment conditions with a low trajectory spread are caused by pilots performing the task in a consistent manner. A large trajectory spread indicates diverse, nonuniform pilot reactions. Figure 26 shows the average trajectory spread per experiment condition.

Normality is rejected in 3/12 cases, and parametric tests are used. There is no significant effect of display, visibility, or (off-)nominal situation on the mean trajectory spread for the whole maneuver; and $p > 0.03$ for every effect and interaction. However, when analyzing only off-nominal situations (in which case normality is rejected in 3/6 cases), visibility has a significant effect on trajectory spread $[\chi^2(1, 66) = 8.3749, p < 0.01]$. This effect is also visible in the separate maneuver stages. There are no significant effects when analyzing all conditions together, but a significant effect of visibility becomes apparent during off-nominal situations during pull-up and descent $[\chi^2(1, 66) = 7.99, p < 0.01; \chi^2(1, 66) = 4.31; p = 0.038]$. However, this does not occur during flyover, $\chi^2(1, 66) = 7.79$, $p < 0.01$.

Encountering low visibility or an off-nominal situation separately does not seem to impact the trajectory spread. However, encountering both at the same time consistently decreases the variability of the flown maneuver trajectories. The combination of the two adverse effects caused the pilots to fly closer to the edge of maneuver possibilities by pulling up at a later time, and therefore caused the trajectories to be grouped closer together.

I. Velocity at Peak

Instead of computing an average, RMSE deviation from the target speed, the momentary speed at maximum altitude is investigated here. If this speed is close to the target of 60 kt, the pilot is able to concentrate on managing his/her speed even while avoiding the obstacle. If it is below 60 kt, it presumably means that the pilot either chose or was forced to prioritize avoiding the obstacle, accepting a loss of speed in the process. Figure 27 shows box plots of the speed at peak altitude, averaged per pilot. Normality is rejected in 4/12 cases. The employed nonparametric tests reveal no significant effects in the overall analysis ($p > 0.03$ in all cases) or in the nominal/off-nominal subsets ($p > 0.01$ in all cases). Off-nominal situations seem to increase the spread of the data, but the median is not significantly affected.
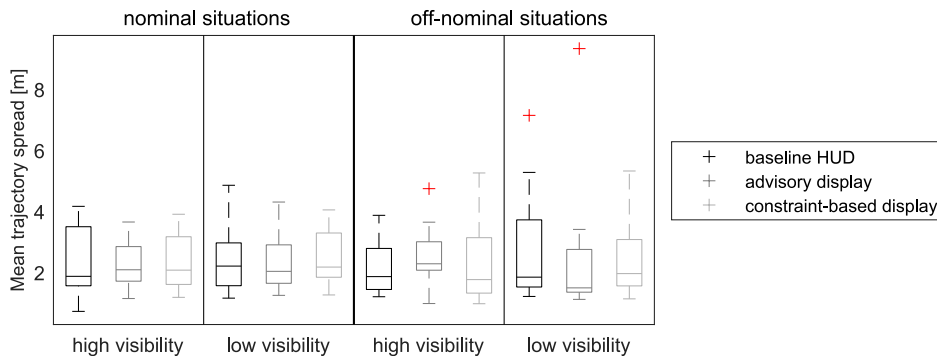

Fig. 26 Box plots of within-pilot trajectory spread per visibility, display, and situation.
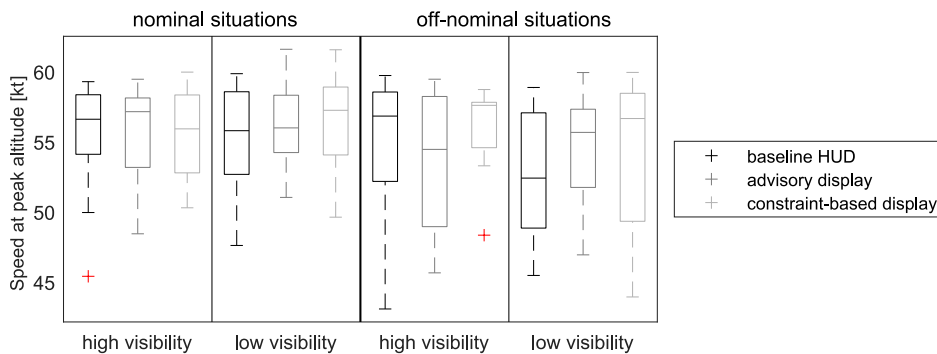

Fig. 27 Box plots of speed at peak altitude per visibility, display, and situation.

J. Tau Analysis

To further analyze the employed pull-up control strategy, a parameter estimation of a prescribed *constant-acceleration* τ-guided maneuver is performed for every pull-up maneuver; see Fig. 19. The guides are computed based on previous work by Padfield [29]. The maneuver time T, the maneuver flight-path angle gap γ_{gap}, and the coupling constant k are estimated.

The pull-up maneuver is identified as the first stretch of data points with a positive change of flight path of $\dot{\gamma} > 0$ after the previously identified maneuver start. The maneuver ends when $\dot{\gamma}$ once again reaches a value of zero for the first time. The maneuver time of $T = t_{\text{end}} - t_{\text{start}}$ and the flight-path angle gap of $\gamma_{\text{gap}} = \gamma(t_{\text{end}}) - \gamma(t_{\text{start}})$ are computed based on the difference in the time and the flight-path angle between the start and end of the maneuver.

To estimate the coupling parameter k, the τ trajectory of the actual flown maneuver as well as the constant-acceleration intrinsic τ guide have to be computed because the coupling parameter k is defined through the relationship between τ_{maneuver}, the instantaneous time to contact of the actually flown maneuver, and τ_{guide} (the prescribed τ guide):

$$\tau_{\text{maneuver}} = k \cdot \tau_{\text{guide}} \tag{5}$$

where τ_{maneuver} is defined as the instantaneous time to contact between the maneuver flight-path angle and its final value. Per convention, γ_{end} is defined as 0 deg, whereas γ_{start} has a negative value. Note that γ_{maneuver} therefore starts at a negative value and approaches zero throughout the maneuver:

$$\gamma_{\text{maneuver}}(t) = -(\gamma_{\text{end}} - \gamma_{\text{start}}) + \gamma(t) \tag{6}$$

Also, $\dot{\gamma}_{\text{maneuver}}$ is simply calculated as the time derivative of γ_{maneuver} because γ_{start} and γ_{end} are constant:

$$\dot{\gamma}_{\text{maneuver}}(t) = \dot{\gamma}(t) \tag{7}$$

Note that τ_{maneuver} can now be calculated through

$$\tau_{\text{maneuver}}(t) = \frac{\gamma_{\text{maneuver}}(t)}{\dot{\gamma}_{\text{maneuver}}(t)} \tag{8}$$

The constant-acceleration τ guide, as given by Padfield [29], is

$$\tau_{\text{guide}}(\hat{t}) = -\frac{T}{2}\left(\frac{1}{\hat{t}} - \hat{t}\right) \tag{9}$$

with the normalized maneuver time of $0 \leq \hat{t} \leq 1$:

$$\hat{t} = \frac{t - t_{\text{start}}}{t_{\text{end}} - t_{\text{start}}} \tag{10}$$

To estimate k, a least-square fit is applied to subsets of the maneuver data. Work by Lu et al. [30] has shown that this approach has a number of downsides, e.g., a sensitivity to maneuver length, boundary conditions causing instability, and sensitivity to incomplete or oscillatory data. In this experiment, however, the analyzed flight-path angles show little to no oscillatory behavior, and the employed methodology seems to provide reasonable results. Therefore, in this experiment, the aforementioned least-square fit methodology is chosen.

The least-square fit is initiated with three data points at the end of the maneuver. The analysis is repeated for every subset of data from three data points up until all data points within the range of $0.2 \leq \hat{t} \leq 1$. In the region close to $\hat{t} = 0$, the τ guide approaches minus infinity. To avoid an influence of this limit behavior on the identification of k, at most, the last 80% of the maneuver is used. The final identified value of k is then chosen as the identified value of the least-square fit with the biggest number of data points that still provide an adjusted $R^2 > 0.97$. Figure 28 shows an example maneuver and fit τ trajectory.

Box plots of the maneuver time T are shown in Fig. 29. Normality is not rejected, and a three-way ANOVA does not reveal any significant effects. Likewise, analyzing nominal and off-nominal situations separately does not reveal any significant effects either.
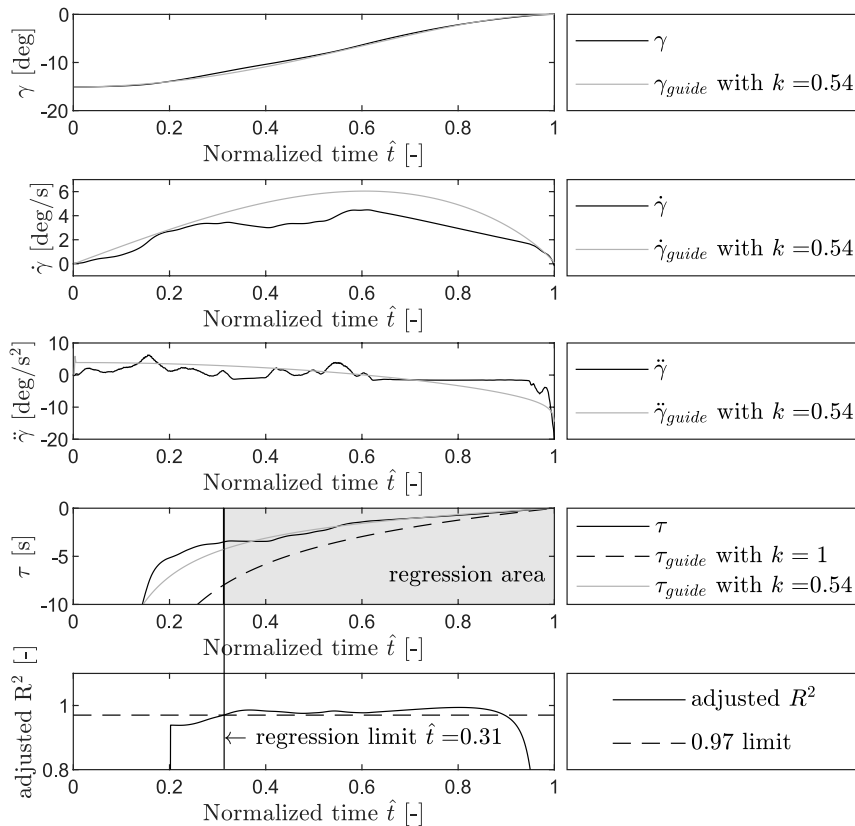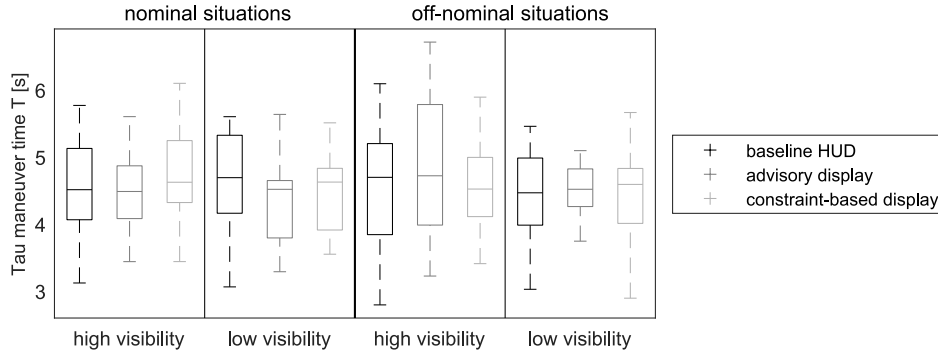

Fig. 28   Example γ trajectory and τ fit.

Fig. 29 Box plots of tau maneuver time *T* per visibility, display, and situation.

The τ-maneuver time T seems to be largely independent from the experiment conditions.

Figure 30 depicts box plots of the maneuver gap γ_{gap}. Normality is not rejected, parametric tests are used. Visibility [$F(1, 134) = 7.74, p < 0.01$] and (off-)nominal situation [$F(1, 134) = 15.63, p < 0.001$] significantly affect the maneuver gap. There is also a significant interaction effect between visibility and (off-)nominal situation $F(1, 134) = 8.28, p < 0.01$. Analyzing nominal situations separately, however, reveals no significant effects; the observed significant effects are caused solely by an increase of the maneuver gap in off-nominal situations and low visibility, which are revealed by a significant effect of visibility when analyzing only off-nominal situations: $F(1, 66) = 13.34, p < 0.001$. Mirroring previous results, only the combination of off-nominal situations and low visibility causes a significant change in the dependent measure. An increase in maneuver gap implies a larger change of γ in the initial pull-up maneuver. This makes sense because the reduced obstacle detection distance necessitates a larger trajectory change in a shorter maneuvering distance to still clear the obstacle.

The employed display seems to only have a small influence on the maneuver gap γ_{gap} in specific conditions; e.g., the advisory display

seems to cause a smaller maneuver gap in nominal low-visibility situations than the other displays. These differences are not significant, however, and not applicable in all conditions.

Figure 31 shows box plots of the coupling parameter k averaged per pilot. The larger the value of k, the later in the maneuver the peak acceleration occurs; at values of $k > 0.5$, the acceleration guide becomes minus infinity at the end of the maneuver, practically meaning that the guide overshoots the target. The only significant effect can be observed when analyzing only off-nominal situations: in that case, visibility significantly affects the coupling constant k [$F(1, 66) = 7.45, p = 0.01$]. An increase of the coupling constant k makes sense when coupled with the requirement to quickly change the flight-path angle when an obstacle appears at close range, as compared to the calmer maneuvers in the other conditions.

K. Pilot Preference

After the experiment, the pilots indicated their confidence in using the different displays to fulfill the task on a scale from one (low) to seven (high), as shown in Table 7 and Fig. 32. In general (i.e., not differentiating between nominal and off-nominal situations), pilots felt most confident using the baseline HUD (6.08) and the advisory
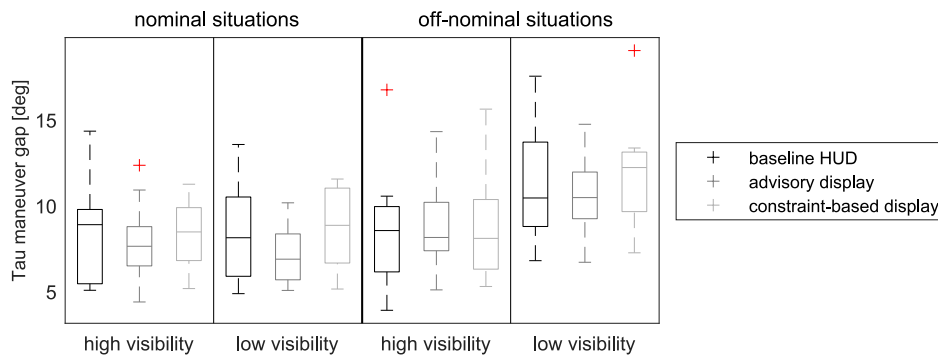

Fig. 30 Box plots of tau maneuver gap γ_{gap} per visibility, display, and situation.
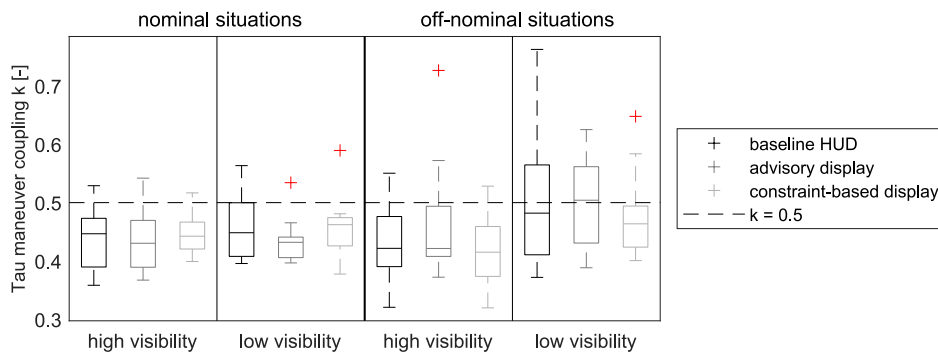

Fig. 31 Box plots of tau-coupling parameter *k* per visibility, display, and situation.

Table 7   Averaged questionnaire result to the question "How confident did you feel while using the baseline/advisory/constraint-based display to fulfill the task?" on a scale from 1 (low) to 7 (high)

Confidence	Baseline HUD	Advisory display	Constraint-based display
General	6.08	5.83	4.92
Nominal	——	6.17	5.00
Off-nominal	——	4.42	4.92

display (5.83), followed by the constraint-based display (4.92). This difference between displays is insignificant; however, $F(2, 33) = 2.35$, $p = 0.11$.

At a significance level of $\alpha = 0.05$, a two-way ANOVA covering two display conditions (advisory and constraint-based) and two situational conditions (nominal and off-nominal) reveals a significant effect of the (off-)nominal situation on the pilot rating [$F(1, 44) = 5.07$, $p < 0.05$], as well as a significant interaction effect [$F(1, 44) = 4.19$, $p < 0.05$]. Whereas the average pilot rating for the constraint-based display remains relatively constant between nominal and off-nominal situations (5.00 and 4.92, respectively), the rating for the advisory display drops significantly from 6.17 to 4.42. Whereas pilots prefer the advisory display in nominal situations, they slightly prefer the constraint-based display in off-nominal situations.

It is interesting to note that the observed drop in confidence when using the constraint-based display in all situations, as well as specifically in nominal situations, seems to stem completely from pilots with less than 1000 flight hours, as shown in Fig. 32. Although the number of pilots with more than 1000 flight hours is rather low, these results could suggest that a larger flight experience enables the pilots to more confidently use the constraint-based display.

V.   Discussion

This experiment investigated the effect of employing a classical advisory display and a constraint-based display during helicopter obstacle avoidance in forward flight. Workload and situation awareness metrics are significantly affected by visibility, in accordance with the hypotheses. Whereas the constraint-based display decreases workload and increases situation awareness according to expectations in all visibility conditions, the advisory display improves the measures only in good visibility. In low visibility, it actually decreases the median situation awareness. Contrary to the hypotheses, the constraint-based display reduces workload and increases situation awareness more strongly than the advisory display. This is surprising because constraint-based displays typically require more information integration from the pilot [13]. However, these results fit the pattern of the questionnaire answers to the pilot's confidence during off-nominal events in Table 7: in off-nominal situations, the constraint-based display is rated with an average score of 4.92, which is higher than the score of the advisory display in the same situations (4.42). A (subconscious) focus on the more memorable, unexpected events while filling out the questionnaires could explain these values. For future research, it will prove valuable to collect ratings like these separately for nominal and off-nominal

situations. A second possible explanation for this finding could be the higher importance of the out-of-window view for general helicopter control as compared to the more instrument-focused fixed-wing approach. Any display information that can be directly related and better conforms to the outside view (like the constraint-based display) might be preferred as compared to other, nonconformal information (like the arrow of the advisory display).

The performance, safety, and control strategy are all mostly impacted by the combination of low visibility and the off-nominal situation. This worst-case situation causes less altitude and lateral deviation, which can be interpreted as flying a more uniform maneuver with less maneuver spread, which is closer to the maneuver limitations and with a smaller safety clearance above the obstacle. Speed deviation increases, but only after the obstacle is cleared: as a result of the more aggressive pull-up maneuver, the recovery to an optimal flight path takes longer. The computed pull-up location and τ-maneuver parameters confirm the expectation that in this worst-case scenario, a later pull-up coincides with a more aggressive pull-up maneuver, which covers a greater change of flight-path angle to still clear the obstacle. Some pilots commented that the support displays enable them to pull up at a later time, as well as at a more consistent location, but other pilots reported no change in perceived behavior at all. The data do not show clear effects of the displays in this regard.

The percentage of unsafe clearances follows this trend, with an increase of unsafe clearances in off-nominal situations. The advisory display presents an exception to this: when encountering an off-nominal situation in low visibility, the number of unsafe clearances actually decreases. A possible explanation for this could be an over-compensating pull-up maneuver, clearing the obstacle at a higher clearance than required and causing a larger speed and altitude deviation as a result. However, the performance measures do not reflect this expectation. The advisory display does cause a decrease of situation awareness in low-visibility situations; it could be hypothesized that the increase in safety in this condition was "paid for" with some increased mental effort, which in turn led to a decrease in mental capacity to maintain the situation awareness level. The baseline HUD causes the most unsafe trajectories when encountering unexpected events, showcasing the positive impact of any of the support displays in these situations. The constraint-based display appears to increase the resilience of the pilot–vehicle system against unexpected events the most, considering the number of unsafe clearances: in three out of four cases, the constraint-based display caused the least unsafe clearances.

For the experiment setup, these results indicate that the difference between nominal and off-nominal situations in high visibility was not substantial enough to elicit a significant change of the dependent measures. Conversely, in nominal situations, the difference between high- and low-visibility conditions was also small. This was probably caused by the inclusion of the contour box around approaching obstacles, which set the effective detection distance to 300 m across all conditions, except the worst-case scenario of low-visibility and off-nominal events. Combined with the already cue-rich baseline HUD and outside visuals, the pilots received an abundance of information in all conditions but the worst, which would explain the insignificant effects of the displays in these conditions. Pilot comments support this argument: occasionally, some pilots would ignore
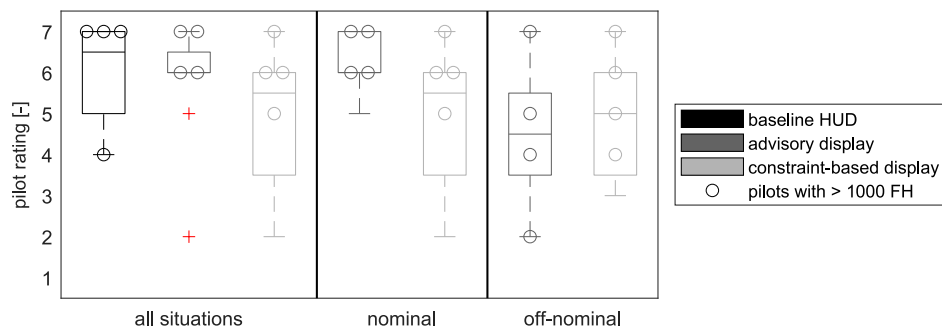
Fig. 32   Box plots of pilot ratings in all, nominal, and off-nominal situations. (FH denotes flight hours.)

the support displays completely, and they only focused on the outside visuals and baseline HUD elements.

Considering pilot preference, the results of this paper are in line with the aforementioned ecological design research in the fixed-wing domain [19]: pilots prefer conventional advisory support systems in nominal situations, but their preference shifts to constraint-based support displays in off-nominal unexpected situations. This can be explained by the kind of information that is communicated to the pilot, even in the event of an off-nominal event: the constraint-based display still provides information about the internal maneuver constraints to the pilot. The advisory display does not provide any information until the obstacle is detected.

The advisory display provides easy-to-follow guidance on how to achieve an "optimal" target trajectory, but it depends on the correct detection and computation of all required data: the internal maneuver constraints, the external environment constraint, and their combination. The constraint-based display communicates only the internal maneuver constraints to the pilots; they have to acquire the external environment constraints themselves and allocate cognitive resources to derive meaning from them. This would explain why the constraint-based display is preferred in off-nominal situations. When the obstacle detection system is not functioning [i.e., it fails to support the perception of the external environment constraint (by drawing the safety zone above an obstacle)], pilots can still use the other half of the constraints (the internal maneuver constraints) to support their decision making, leading to a more "robust" control performance.

The differences between the investigated displays are not statistically significant. There are some effects on the workload, situation awareness, and pilot preference, but they do not afford a general conclusion concerning positive or negative effects of the displays on objective performance or safety measures. Possibly reasons for this are as follows:

1) The pilots were well able to maintain an adequate level of performance and safety across all display conditions; the only difference is a change of required mental effort. The displays might have helped the pilots in reducing the required mental effort to perform the task, but the actual task performance stayed level.

2) The analyzed task is too focused on short-term inner-loop control to reveal big differences, and the baseline HUD and outside visibility already provide all information that helicopter pilots use to perform the analyzed task, even in off-nominal situations. The displays only provided additional information that pilots might or might not have used. Especially in hectic fast-paced maneuvers or reactions

to obstacles, it seems plausible that pilots concentrated on the source of information they are most familiar with: the outside visuals.

3) The analyzed displays are quite similar to each other because they are both based on the maximum effective climb angle γ_{limit}. This was a deliberate experiment design decision to focus more on the different data representation philosophies and less on differences in the actual data being displayed. Using different data sources and constraint calculations for the displays might incur greater differences, but it also introduces the question as to which part of the display made the difference: the data itself, or its representation. In addition, the accuracy of the parameters used to calculate γ_{limit} could be improved. For example, the current pilot reaction-onset time delay is based on a one-degree-of-freedom experiment, and not on actual helicopter pilot performance during obstacle avoidance.

4) The display design of both variants (e.g., color, symbology, location) was rather basic as compared to current developments in helicopter HUD applications, as shown by, e.g., Münsterer et al. [6]. Improving display design aspects could increase the effect of the investigated displays. However, care has to be exerted to improve both displays to a very similar extent. Otherwise, the obtained results could be influenced more by these differing display design characteristics and less by the different data representation mode, which was the focus of this experiment.

5) The performed task was monotonous and repetitive. Even the unexpected off-nominal situations became predictable after a few occurrences; and the first encountered unexpected events, where pilots might have been most surprised, occurred during the training phase of the experiment. Even though it was never clear to the pilot *when* an obstacle might not be detected in time, they were aware that this late detection would happen eventually and regularly, that there were no other unexpected events, and that a climb-over maneuver would be the only feasible avoidance trajectory. Even if positive influences of the constraint-based display were assumed, the obstacles and possible avoidance trajectories in this experiment lacked a sufficient amount of variability (and the off-nominal situations a sufficient amount of "unexpectedness") to trigger those advantages.

6) Lastly, a higher number of pilot participants might increase the power of the employed test statistics, provided the results show the same trends. The number of 12 participants and the within-participants experiment design enabled the use of parametric tests, but at the cost of lower power.

To remedy these problems, future experiments investigating obstacle avoidance support systems should incorporate a higher variability of obstacles and possible avoidance trajectories, more
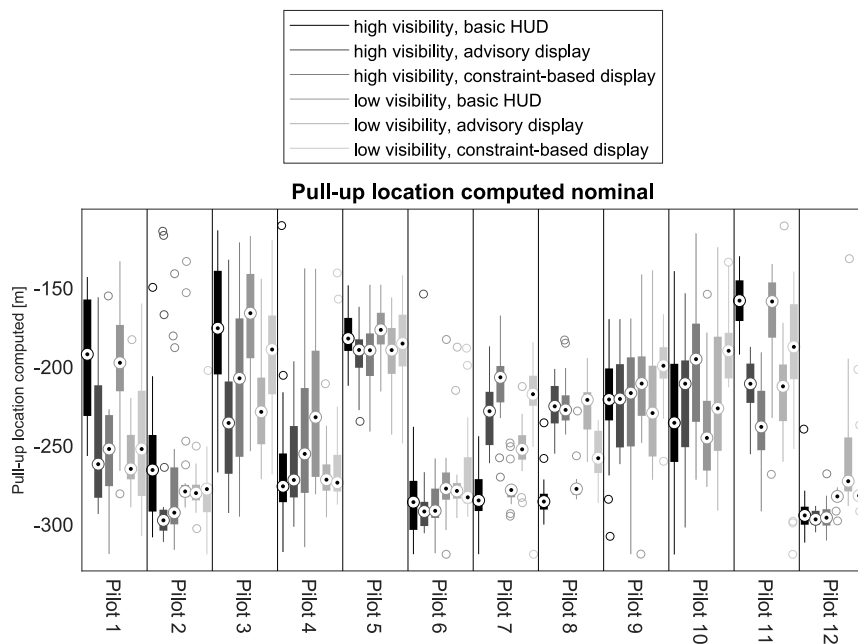

Fig. 33   Box plots of computed pull-up location per visibility, display, and situation, separated per pilot.

varied approach speeds and tasks (e.g., hovering in obstructed areas, or approaching confined areas), and larger differences between display and visibility conditions. Off-nominal events should be designed such that neither their occurrence nor the proper control response can be easily predicted by the participating pilots.

This study focused on the effect of the advisory and constraint-based head-up support systems. The assumption was made that any HUD system that can include such displays would, as a standard, also show a baseline HUD with primary flight data, which is why this was chosen as the baseline condition. However, the inclusion of a condition without any HUD elements, only relying on outside visuals, could provide insight into the effects of employing a baseline HUD and would enable the comparison of highly augmented conditions (HUD with advisory or constraint-based display) with nonaugmented display conditions.

It is important to note that many results were not consistently found across all pilots, as Fig. 33 illustrates in the case of the computed pull-up location. Whereas the pull-up locations of some pilots were clearly impacted by the employed display (e.g., pilot 3 or pilot 7), other pilots were not impacted much by display or visibility (for example, pilots 5 and 6). Although there seem to be individual preferences and different reactions to the employed displays, these reactions were not uniform and cannot be extrapolated to all experiment participants, let alone the general helicopter pilot population. Considering these widespread responses, an advisory display that emphasizes one specific target trajectory does not seem to be able to accommodate different pilot preferences and strategies. A constraint-based or ecological interface, on the other hand, could still provide support even to pilots with different control preferences because it emphasizes only the systemic and environmental limitations; the pilots are encouraged to decide for themselves how to control the system, enabling and supporting more diverse strategies between pilots.

Improving subjective measures can be seen as a first step toward EID-based support systems in helicopters that are 1) seen favorable by pilots, by positively impacting "subjective" workload and situation awareness measures; and 2) significantly affect "objective" task performance and safety measures. Whereas the first step has been reached in this experiment, follow-up research should investigate the properties of helicopter automation systems that can improve both subjective and objective measures concurrently. Of special interest is a scenario with a longer time frame, requiring more rule- and knowledge-based pilot control.

VI. Conclusions

Two helicopter obstacle avoidance displays were evaluated during low-altitude forward flight: an advisory display and a constraint-based display. Results show the employed support displays decreased subjective ratings of workload and increased subjective ratings of situation awareness, with the constraint-based display causing larger effects. Confirming the current hypothesis, pilots preferred the advisory display in nominal situations and the constraint-based display in off-nominal situations. Although the constraint-based display seems to be the most robust display concerning safety during off-nominal events, differences were not significant. The improved subjective ratings showcase the employed displays' potential to improve the pilots' experience while performing obstacle avoiding tasks. However, contrary to expectations, the displays in this experiment setup did not elicit significant changes in task performance or safety.
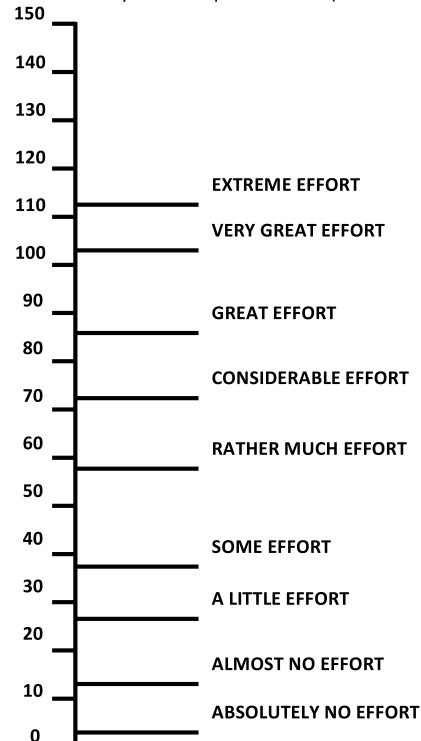
Appendix: Experiment Questionnaires

SART (Situation Awareness Rating Scale)

Please rate the level of each component of situation awareness that you had when you performed the task (without sensor failure) by circling the appropriate number for each component.

DEMAND									
Instability of situation Likeness of the situation to change suddenly	Low	1	2	3	4	5	6	7	High
Variability of situation Number of variables that require your attention during the task	Low	1	2	3	4	5	6	7	High
Complexity of situation Degree of complication (number of closely connected or coupled elements) of the situation	Low	1	2	3	4	5	6	7	High

SUPPLY									
Arousal Degree to which you are ready for activity; ability to anticipate and keep up with the flow of events	Low	1	2	3	4	5	6	7	High
Spare mental capacity Amount of free mental capacity available during the task to apply to new and different tasks	Low	1	2	3	4	5	6	7	High
Concentration Degree to which your thoughts are brought to bear on the situation; degree to which you focus on important elements and events	Low	1	2	3	4	5	6	7	High
Division of attention Ability to divide your attention among several key issues during the mission; ability to concern yourself with many aspects of current and future events simultaneously	Low	1	2	3	4	5	6	7	High

UNDERSTANDING									
Information quantity Amount of knowledge received and understood (e.g. attitude, aircraft & obstacle position, speed and direction of flight, information about future aircraft states)	Low	1	2	3	4	5	6	7	High
Information quality Degree of goodness, value, usefulness of information communicated	Low	1	2	3	4	5	6	7	High
Familiarity Degree of acquaintance with the situation	Low	1	2	3	4	5	6	7	High

RSME (Rating Scale Mental Effort)

Please indicate, by marking the vertical axis below, how much effort it took for you to complete the task (without sensor failure).

```
150
140
130
120
110 ── EXTREME EFFORT
    ── VERY GREAT EFFORT
100
90  ── GREAT EFFORT
80  ── CONSIDERABLE EFFORT
70
60  ── RATHER MUCH EFFORT
50
40  ── SOME EFFORT
30  ── A LITTLE EFFORT
20
    ── ALMOST NO EFFORT
10
    ── ABSOLUTELY NO EFFORT
0
```

Code

Comments

Please see the backside of this questionnaire.

Fig. A1 Questionnaire filled out by participating pilots after each condition (front side).

Comments

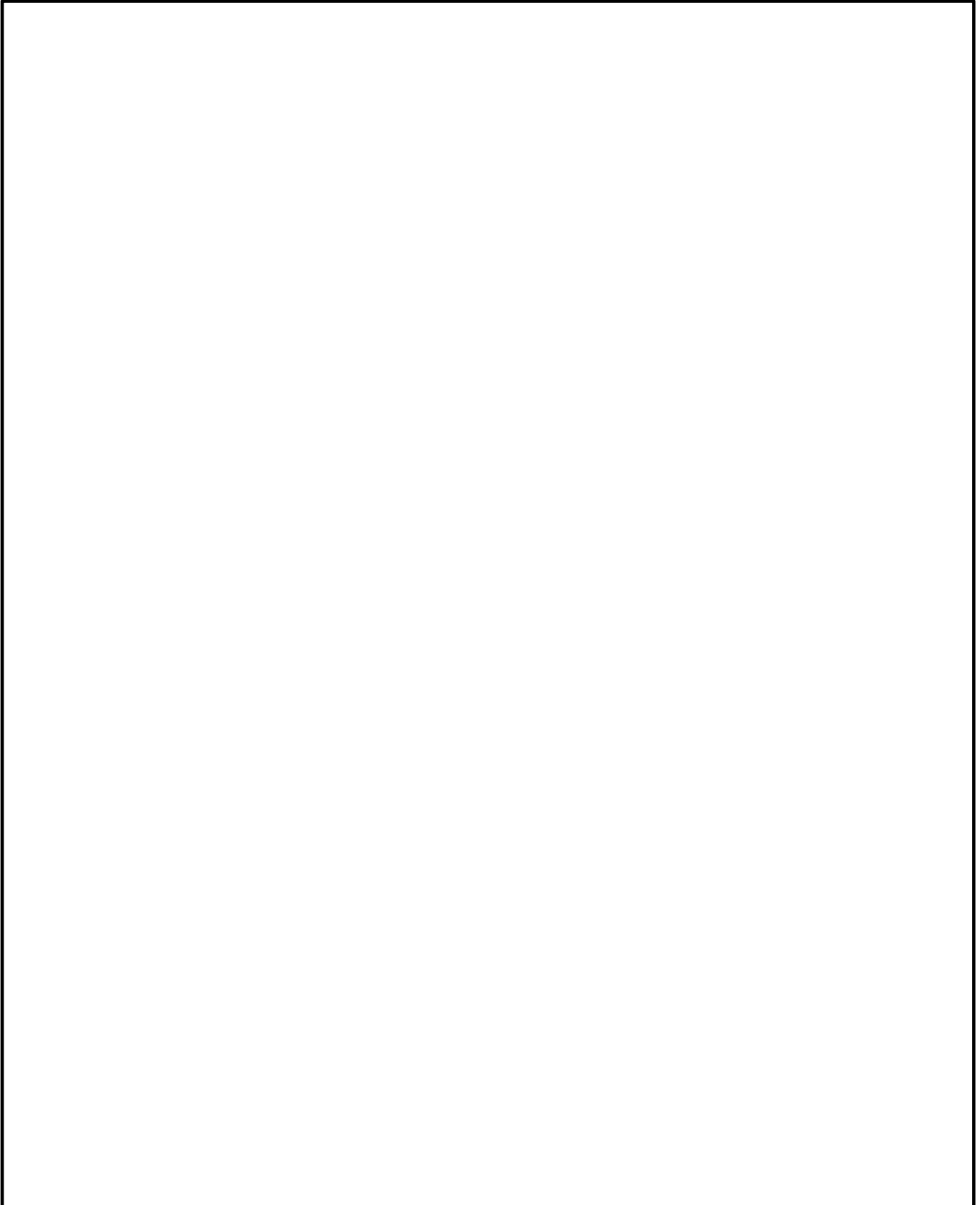Do you have additional comments? Please note them below.

Fig. A2   Questionnaire filled out by participating pilots after each condition (backside).

Baseline HUD

How confident did you feel in using only the outside visuals, the baseline head-up display (HUD), and the obstacle boxes to fulfil the task?	Low	1	2	3	4	5	6	7	High

Do you have additional comments on the simulation realism, the outside visuals or the baseline head-up display?

Arrow symbology

In general, how confident did you feel in using the arrow symbology to fulfill the task?	Low	1	2	3	4	5	6	7	High
In cases **without faults**, how confident did you feel in using the arrow symbology to fulfill the task?	Low	1	2	3	4	5	6	7	High
In cases **with faults**, how confident did you feel in using the arrow symbology to fulfill the task?	Low	1	2	3	4	5	6	7	High

Do you have any additional comments on the arrow symbology?

Steepest climb symbol

In general, how confident did you feel in using the steepest climb symbol to fulfill the task?	Low	1	2	3	4	5	6	7	High
In cases **without faults**, how confident did you feel in using the steepest climb symbol to fulfill the task?	Low	1	2	3	4	5	6	7	High
In cases **with faults**, how confident did you feel in using the steepest climb symbol to fulfill the task?	Low	1	2	3	4	5	6	7	High

Do you have any additional comments on the steepest climb symbol?

Fig. A3   Questionnaire filled out by participating pilots after the experiment.

References

[1] Anon., "Safety Report (August 2020)," Tech. Rept., U.S. Helicopter Safety Team, 2020, https://ushst.org/reports/.

[2] Anon., "Annual Safety Review 2019," European Union Aviation Safety Agency TR TO-AA-19-001-EN-N, Cologne, Germany, 2019. https://doi.org/10.2822/098259

[3] Anon., "Final Report—EHEST Analysis of 2000-2005 European Helicopter Accidents," Tech. Rept., European Helicopter Safety Team, 2010.

[4] Anon., "Final Report—EHEST Analysis of 2006-2010 European Helicopter Accidents," Tech. Rept., European Helicopter Safety Team, 2015.

[5] Szoboszlay, Z. P., McKinley, R. A., Braddom, L. S. R., Harrington, W. W., Burns, H. N., and Savage, J. C., "Landing an H-60 Helicopter in Brownout Conditions Using 3D-LZ Displays," *Proceedings of the American Helicopter Society 66th Forum*, AHS Paper 122, 2010. https://doi.org/10.13140/2.1.3725.3764

[6] Münsterer, T. R., Singer, B., Zimmermann, M., and Gestwa, M., "NIAG DVE Flight Test Results of LiDAR Based DVE Support Systems," *Degraded Environments: Sensing, Processing, and Display 2018*, edited by J. N. Sanders-Reed, and J. J. Arthur, III, Vol. 10642, SPIE, Bellingham, WA, 2018, Paper 106420I. https://doi.org/10.1117/12.2305714

[7] Funabiki, K., Tsuda, H., Shimizu, A., Sugihara, Y., Tawada, K., and Hasebe, K., "Objective Flight Evaluation of Visual Cue for DVE Helicopter Operation," *AIAA SciTech 2020 Forum*, AIAA Paper 2020-0055, 2020. https://doi.org/10.2514/6.2020-0055

[8] Minor, J., Morford, Z., and Harrington, W., "Sensor Data/Cueing Continuum for Rotorcraft Degraded Visual Environment Operations," *Degraded Environments: Sensing, Processing, and Display 2017*, edited by J. N. Sanders-Reed, and J. J. Arthur, III, Vol. 10197, SPIE, Bellingham, WA, 2017, Paper 101970Y. https://doi.org/10.1117/12.2262939

[9] Kahana, A., "Obstacle-Avoidance Displays for Helicopter Operations: Spatial Versus Guidance Symbologies," *Journal of Aerospace Information Systems*, Vol. 12, No. 7, 2015, pp. 455–466. https://doi.org/10.2514/1.I010306

[10] Godfroy-Cooper, M., Szoboszlay, Z., Kahana, A., and Rottem-Hovev, M., "Terrain and Obstacle Avoidance Displays for Low-Level Helicopter Operations in Degraded Visual Environments," *Proceedings of the American Helicopter Society 72nd Forum*, AHS Paper 308, 2016.

[11] Godfroy-Cooper, M., Miller, J. D., Bachelder, E., and Wenzel, E. M., "Isomorphic Spatial Visual-Auditory Displays for Operations in DVE

for Obstacle Avoidance," *Proceedings of the 44th European Rotorcraft Forum*, Paper 94, Delft, The Netherlands, 2018.

[12] Walters, R., McCandless, J., and Feigh, K. M., "Pilot Cueing for Rotorcraft Shipboard Landings," *AIAA SciTech 2020 Forum*, AIAA Paper 2020-0056, 2020.
https://doi.org/10.2514/6.2020-0056

[13] Van Paassen, M. M., Borst, C., Ellerbroek, J., Mulder, M., and Flach, J. M., "Ecological Interface Design for Vehicle Locomotion Control," *IEEE Transactions on Human-Machine Systems*, Vol. 48, No. 5, 2018, pp. 541–555.
https://doi.org/10.1109/THMS.2018.2860601

[14] Vicente, K. J., and Rasmussen, J., "The Ecology of Human-Machine Systems II: Mediating "Direct Perception" in Complex Work Domains," *Ecological Psychology*, Vol. 2, No. 3, 1990, pp. 207–249.
https://doi.org/10.1207/s15326969eco0203_2

[15] Vicente, K. J., and Rasmussen, J., "Ecological Interface Design: Theoretical Foundations," *IEEE Transactions on Systems, Man, and Cybernetics*, Vol. 22, No. 4, 1992, pp. 589–606.
https://doi.org/10.1109/21.156574

[16] Comans, J., "Visualizing Rules, Regulations, and Procedures in Ecological Information Systems," Ph.D. Thesis, Delft Univ. of Technology, Delft, The Netherlands, 2017.
https://doi.org/10.4233/UUID:9B3F9BB6-EF1B-41ED-803A-7E7976784B85

[17] Borst, C., Flach, J. M., and Ellerbroek, J., "Beyond Ecological Interface Design: Lessons From Concerns and Misconceptions," *IEEE Transactions on Human-Machine Systems*, Vol. 45, No. 2, 2015, pp. 164–175.
https://doi.org/10.1109/THMS.2014.2364984

[18] Jenkins, M. P., Hogan, C., and Kilgore, R., "Ecological Display Symbology to Support Pilot Situational Awareness During Shipboard Operations," *Proceedings of the 2015 IEEE International Multi-Disciplinary Conference on Cognitive Methods in Situation Awareness and Decision*, Inst. of Electrical and Electronics Engineers, New York, 2015, pp. 213–219.
https://doi.org/10.1109/COGSIMA.2015.7108200

[19] Borst, C., Mulder, M., and Van Paassen, M. M., "Design and Simulator Evaluation of an Ecological Synthetic Vision Display," *Journal of Guidance, Control, and Dynamics*, Vol. 33, No. 5, 2010, pp. 1577–1591.
https://doi.org/10.2514/1.47832

[20] Padfield, G., Dequin, A.-M., Haddon, D., Kampa, K., Basset, P.-M., von Grünhagen, W., Haverdings, H., and McCallum, A., "Predicting Rotorcraft Flying Qualities Through Simulation Modelling. A Review

of Key Results from GARTEUR AG06," *Proceedings of the 22nd European Rotorcraft Forum*, 1996.

[21] Hosman, R. J. A. W., and Stassen, H. G., "Pilot's Perception and Control of Aircraft Motions," *IFAC Proceedings Volumes*, Vol. 31, No. 26, 1998, pp. 311–316.
https://doi.org/10.1016/S1474-6670(17)40111-X

[22] Stroosma, O., van Paassen, M. M., and Mulder, M., "Using the SIMONA Research Simulator for Human-Machine Interaction Research," *AIAA Modeling and Simulation Technologies Conference and Exhibit*, AIAA Paper 2003-5525, 2003.
https://doi.org/10.2514/6.2003-5525

[23] Miletović, I., Pool, D. M., Stroosma, O., Pavel, M. D., Wentink, M., and Mulder, M., "The Use of Pilot Ratings in Rotorcraft Flight Simulation Fidelity Assessment," *Proceedings of the American Helicopter Society 73rd Forum*, 2017.

[24] Zijlstra, F. R. H., and Van Doorn, L., "The Construction of a Scale to Measure Perceived Effort," Tech. Rept., Delft Univ. of Technology, Delft, The Netherlands, 1985.

[25] de Waard, D., "The Measurement of Drivers' Mental Workload," Ph.D. Thesis, Univ. of Groningen, Groningen, The Netherlands, 1996.

[26] Taylor, R. M., "Situational Awareness Rating Technique (SART): The Development of a Tool for Aircrew Systems Design," *Proceedings of the AGARD AMP Symposium on Situational Awareness in Aerospace Operations*, CP478, Seuilly-sur Seine, France, NATO AGARD, 1989.

[27] Padfield, G. D., Clark, G., and Taghizad, A., "How Long Do Pilots Look Forward? Prospective Visual Guidance in Terrain-Hugging Flight," *Journal of the American Helicopter Society*, Vol. 52, No. 2, 2007, pp. 134–145.
https://doi.org/10.4050/JAHS.52.134

[28] Scaramuzzino, P. F., Pavel, M. D., Pool, D. M., Stroosma, O., Mulder, M., and Quaranta, G., "Effects of Helicopter Dynamics on Autorotation Transfer of Training," *Journal of Aircraft* (Under Review).

[29] Padfield, G. D., "The Tau of Flight Control," *Aeronautical Journal*, Vol. 115, No. 1171, 2011, pp. 521–556.
https://doi.org/10.1017/S0001924000006187

[30] Lu, L., Jump, M., and Jones, M., "Tau Coupling Investigation Using Positive Wavelet Analysis," *Journal of Guidance, Control, and Dynamics*, Vol. 36, No. 4, 2013, pp. 920–934.
https://doi.org/10.2514/1.60015

P. Wei
Associate Editor